5-15-2023

Biomechanical models and mechanisms of cellular morphogenesis and cerebral cortical expansion and folding

David C Van Essen
Washington University School of Medicine in St. Louis

Seminars in Cell and Developmental Biology 140 (2023) 90–104

Contents lists available at ScienceDirect

Seminars in Cell and Developmental Biology

journal homepage: www.elsevier.com/locate/semcdb

Biomechanical models and mechanisms of cellular morphogenesis and cerebral cortical expansion and folding

David C. Van Essen

Department of Neuroscience Washington University School of Medicine, 660S. Euclid, Saint Louis 63110, USA

ARTICLE INFO

Keywords:
Tension
Cytoskeleton
Embryogenesis
Gyrification

ABSTRACT

Morphogenesis of the nervous system involves a highly complex spatio-temporal pattern of physical forces (mainly tension and pressure) acting on cells and tissues that are pliable but have an intricately organized cytoskeletal infrastructure. This review begins by covering basic principles of biomechanics and the core cytoskeletal toolkit used to regulate the shapes of cells and tissues during embryogenesis and neural development. It illustrates how the principle of 'tensegrity' provides a useful conceptual framework for understanding how cells dynamically respond to forces that are generated internally or applied externally. The latter part of the review builds on this foundation in considering the development of mammalian cerebral cortex. The main focus is on cortical expansion and folding – processes that take place over an extended period of prenatal and postnatal development. Cortical expansion and folding are likely to involve many complementary mechanisms, some related to regulating cell proliferation and migration and others related to specific types and patterns of mechanical tension and pressure. Three distinct multi-mechanism models are evaluated in relation to a set of 18 key experimental observations and findings. The Composite Tension Plus (CT+) model is introduced as an updated version of a previous multi-component Differential Expansion Sandwich Plus (DES+) model (Van Essen, 2020); the new CT+ model includes 10 distinct mechanisms and has the greatest explanatory power among published models to date. Much needs to be done in order to validate specific mechanistic components and to assess their relative importance in different species, and important directions for future research are suggested.

1. Introduction

Biological structures acquire their distinctive shapes via the process of morphogenesis - an intricately orchestrated set of molecular, cellular, and tissue-wide events and interactions in which physical forces change the shapes and sizes of individual cells, different brain and body tissue components, and the organism as a whole. Morphogenesis of the nervous system is particularly fascinating because it progresses from a simple geometry early in embryogenesis to an adult organization that is extraordinarily complex and amazingly diverse across species. Moreover, the sizes and shapes of neural cells and tissues can provide useful insights regarding function, as emphasized a century ago by Cajal [2].

My contributions to the study of morphogenesis began serendipitously 25 years ago, arising from a longstanding interest in the structure, function, and development of cerebral cortex. While musing about the process of cortical folding, it occurred to me that mechanical tension in axons connecting nearby cortical regions might help drive the folding process. It soon became apparent that this simple notion had not previously been published, nor had the potential been explored for a much broader role for mechanical tension in neural morphogenesis. In 1997, I published a general tension-based morphogenesis (TBM) hypothesis [3], positing that mechanical tension along axons, dendrites, and glial processes works in concert with mechanical pressure to account for many aspects of nervous system morphogenesis, including why the cortex increases in surface area much more than in thickness and why it becomes convoluted in large-brained animals. An important general corollary is that mechanical tension should keep wiring length short and overall neural circuitry compact. Indeed, minimization of wiring length has long been considered an important principle of nervous system architecture [4–8].

The TBM hypothesis has been widely cited, most commonly in relation to the process of cortical folding. However, many alternative mechanisms for cortical folding have been proposed, both before and after my 1997 paper. As is often the case in developmental biology,

Abbreviations: CGM, cortical gray matter; CMS, Cerebellar Multi-layer Sandwich; CT+, Composite Tension Plus; DES+, Differential Expansion Sandwich Plus; DTE, differential tangential expansion; GBB, Gel-Brain Bilayer; OCL, outer cortical and leptomeningeal; RD, Radial Dispersion; TBM, tension-based morphogenesis.

E-mail address: vanessen@wustl.edu.

https://doi.org/10.1016/j.semcdb.2022.06.007
Received 20 March 2022; Received in revised form 31 May 2022; Accepted 16 June 2022
Available online 13 July 2022

multiple mechanisms very likely operate in concert for a process as complex as cortical folding. In 2020, I reviewed the burgeoning literature since 1997 [1]. This included consideration at a molecular and cellular level of how the intracellular cytoskeleton generates mechanical tension and how tension works against pressure (both osmotic and focally directed) to maintain or modify cell shape. I also reformulated the original tension-based folding hypothesis for cerebral cortex and showed how the five tenets of a new composite 'Differential Expansion Sandwich Plus' (DES+) model account for a wide range of phenomena by invoking a combination of axonal tension (both tethering and pathway-specific), radially biased dendritic tension, tangential tension in the outer cortical leptomeningeal layer, plus other early factors such as differential proliferation and migration. I also proposed a separate Cerebellar Multi-layer Sandwich (CMS) model that can account for many distinctive aspects of cerebellar morphogenesis and adult architecture. Finally, I suggested a wide range of experimental tests that could provide critical evidence for or against specific tenets of the DES+ and CMS models.

The present review revisits the role of mechanical forces in cellular differentiation, early embryogenesis, and cortical expansion and folding. Relative to the previous review [1] it provides expanded coverage of several key topics, while skipping or briefly summarizing others that need little updating. Section 2 presents a cytoskeletal and biomechanical framework for morphogenesis. One objective is to provide an intuitive understanding of how cellular growth can (and cannot) change the shape of soft, highly pliable neural tissue. This is important in order to appreciate why the putative mechanisms proposed in some morphogenetic models are biomechanically implausible, if not impossible. Section 2 also addresses several roles for tension in early embryogenesis, a topic largely untouched in my 2020 review. Section 3 focuses on cerebral cortex, with an emphasis on cerebral cortical expansion and folding. It introduces the Composite Tension Plus (CT+) model, which is a significant refinement of the aforementioned DES+ model [1] that retains the same 5 core tenets but includes additional sub-tenets that highlight the complementarity of multiple mechanisms, including tension along axons, dendrites, and glial cells. It also describes two other prominent multi-component models, the Radial Dispersion (RD) model [9,10] and the Gel-Brain Bilayer (GBB) model [11] and systematically evaluates the ability of all three models and their component mechanisms to account for 18 distinct experimental observations. In brief, the CT+ model has much greater explanatory power than these alternative models. Moreover, criticisms of the axonal tension mechanism have focused largely on a single study [12] in which tissue cut experiments failed to reveal one particular type of axonal tension in a single species. However, there are alternative explanations for these tissue cut observations. The ongoing debate about the relative importance of tension vs other mechanisms in cortical expansion and folding will benefit from considering the much broader range of key observations discussed below.

2. A cytoskeletal and biomechanical framework for morphogenesis

Two seminal concepts that arose outside neuroscience are highly relevant to nervous system morphogenesis. A century ago, D'Arcy Thompson, a pioneer in mathematical biology, proposed that morphogenesis in general is driven by an interplay between mechanical *tension* and *pressure* acting on structures having physical asymmetries and anisotropies [13]. His examples were based on non-neural biological structures, but the principles apply equally well to the developing nervous system. The second concept is the property of *tensegrity* (a condensation of '*tension integrity*'), as promulgated for architecture in the mid-twentieth century by Buckminster Fuller [14] and for cell biology by Donald Ingber [15,16] in recent decades. A tensegrity structure attains stability by having some components under tension and others under compression, rather than the predominantly compressive forces that support conventional buildings. A canonical architectural example is a geodesic dome, where the distribution of struts under tension vs compression depends on external forces (e.g., gravity and wind) and can change rapidly (e.g., when buffeted during a storm). A good molecular example of tensegrity is the aptly named buckminsterfullerene, a 60-carbon-atom molecule whose caged 'soccer-ball' geodesic structure provides mechanical rigidity [17]. At a cellular level, living cells, while generally soft and pliable, are not floppy bags of molecular and macromolecular soup. Rather, they are pressurized and prestressed 'tensegrity structures' with a complex cytoskeletal architecture that is highly responsive to dynamic developmental and environmental forces [18,19].

2.1. Cytoskeletal components

The cytoskeleton includes three major filamentous components – actin filaments, microtubules, and intermediate filaments – plus diverse membrane-bound and transmembrane components that serve as mechanical anchors [20–23]. These core components account for many material properties revealed by passive mechanical perturbations, and they play important roles in cellular force generation and transmission.

- Filamentous actin (*F-actin*) is a polarized filament whose length is dynamically regulated by polymerization of G-actin subunits at one end and depolymerization at the other [20,24,25]. Actin can generate forces through its interactions with various subtypes of *myosin* [26–29] and also through subunit polymerization [23]. Cross-liking of F-actin into various geometric configurations and interactions with diverse cofactors enable actin and actomyosin to play diverse roles in force generation.
- *Alpha-tubulin* and *beta-tubulin* are the dominant subunits of *microtubules*, which are tubular, larger in diameter than F-actin, lengthened via subunit assembly at one end, and shortened by disassembly at the other [30].
- *Neurofilaments (NFs)* and other *intermediate filaments* (IFs) are a diverse set of protein heteropolymers that are intermediate in diameter [23]. In axons, NFs run in cable-like arrays, have sidearm protrusions that interact with other cytoskeletal elements, and contribute to elasticity and the regulation of axon/neurite diameter [31,32].
- A variety of *anchoring molecules* mediate *focal adhesion* of intracellular filaments to transmembrane anchoring molecules in the plasma membrane [20,21,33]. These include *integrins*, which bind externally to the extracellular matrix (ECM) – a complex macromolecular network that occupies interstitial space, including the basal lamina (basement membrane) at the pial surface [34].
- Other key transmembrane entities that add physical integrity include *adherens junctions*, which connect adjacent cells via homophilically binding *cadherins,* and *tight junctions* between epithelial cells, which establish a diffusion barrier critical for maintaining elevated CSF pressure [35], as well as *gap junctions*, *desmosomes*, and *synapses* themselves.

2.2. Forces and material properties

With this 'cytoskeletal toolkit' in mind, Table 1 categorizes key **physical forces** and **material properties** of embryonic and CNS tissue plus exemplar associations with specific cytoskeletal components. Physical forces are classified by their cellular/subcellular vs macroscopic scale, dimensionality (1D or 2D), and whether the force is actively generated or a passive response to an imposed displacement. *Axial tension* occurs when elongated cellular components anchored at both ends are passively stretched, or when a longitudinal shortening force is generated by sliding between filaments (*actomyosin, microtubules)*. *Axial pressure* can be highly anisotropic, but only when cellular components have high bending stiffness as they push (e.g., elongation of bundled

Table 1
Physical forces and material properties in developing CNS tissue.

A. Mechanical forces

- Cellular/subcellular
  - Axial (1D) forces
    - Axial tension
      - passive stretch of anchored filaments (*all types*)
      - force generation (*sliding actomyosin filaments, microtubules*)
    - Axial pressure (*requires high bending stiffness*)
      - polymerization of actin bundles (*filopodia*), microtubule bundles
  - Interface (2D) forces
    - Transmembrane pressure (*elevated intracellular osmotic pressure*)
    - Surface tension
      - passive stretch of plasma membrane and subcellular cortex
      - contraction of actomyosin 'cortex' under plasma membrane
    - Lamellar pressure (*polymerization of actin mesh in lamellopodia*)
- Tissue (macroscopic)
  - Elevated CSF pressure
    - generated by CSF production
    - pressure difference along epithelium bounded by tight junctions
    - counterbalanced by surface tension along diffusion barrier
  - Pressure or tension exerted by neighboring regions and tissues
  - Vascular forces
    - blood pressure pulsations
    - vascular smooth muscle tension

B. Material properties (see SI Topic 1 of ref [1] for published values)

- Elasticity (compliance = 1/stiffness)
  - Tensile or compressive
  - Bending, shear
  - Surface indentation
- Viscosity
- Plastic (non-recovering) behavior
- Adhesiveness (selective adhesion) (Integrins; ECM)

actin filaments in growth cone filopodia and also microtubules) [23,36]. Interface (2D) forces arise at the interface between materials/components, particularly the plasma membrane. *Intracellular osmotic pressure* is regulated by transmembrane transport of ions, water, and other materials handled by a specific molecular subsystem [37]. Elevated intracellular osmotic pressure induces water influx and cell expansion, thereby stretching the plasma membrane. This is counterbalanced by *surface tension* at the plasma membrane (a tangential force striving to reduce the surface area of the interface between hydrophobic and hydrophilic components) and often by additional *interface tension* in regions containing an underlying actin-enriched cytoskeletal 'cortex' [23,29]. Another type of 2D pressure occurs along the margins of lamellopodia – thin cytoplasmic sheets that expand along their outer margin by polymerization of a 2D meshwork of actin filaments [38].

At a tissue level, one major force is the elevated pressure in compartments filled by cerebrospinal fluid (CSF), namely, the embryonic 'vesicles' that arise early in brain development and the ventricles that they later become. Maintaining an elevated pressure depends on having a steady source of CSF pumped into the vesicle/ventricle (by the choroid plexus or its precursors) plus a diffusion barrier based on tight junctions in the tissue lining the fluid compartment. This pressure differential promotes outward bulging of the epithelium, and it is counterbalanced by surface tension along the diffusion barrier. Another important force 'category' is inherently more diverse, as it includes the complex 3D patterns of pressure and tension arising as embryonic CNS tissue grows within a physically constrained environment. Neighboring brain structures may press against one another or against other nearby tissues (e.g., the dura mater), while other macroscopic stresses may include a tensile stretching force. A final force category is related to the brain vasculature, which emerges via angiogenesis early in neural development, starting with invasion of endothelial cells of mesodermal origin [39]. Blood circulation is driven by pulsatile pressure fluctuations and is regulated by arterial and venous smooth muscle. However, aside from the crucial and complex roles of the vasculature in keeping the brain alive and healthy, there are not to my knowledge well characterized influences of vascular forces per se on nervous system morphogenesis.

In terms of *material properties*, embryonic tissue and developing CNS tissue are in general soft and pliable (see SI Topic 1 of ref. [1]), and they grow in an incompressible aqueous fluid environment. Table 1B lists key material (biomechanical) properties that can be assayed in tissues, cells, or molecules and in vivo or in vitro using diverse methods to estimate physical deformation (strain) in response to applied force (stress) [40]. (i) *Elasticity* (*compliance)* and its inverse (*stiffness)* reflect a linear, time-independent component of deformation that can be measured under linearly aligned stress (*tensile* and *compressive stiffness*) or more complex stress configurations (*bending* or *shear stiffness*). *Viscosity* is manifested by a time-dependent displacement under constant force. *Plastic* behavior involves nonelastic deformation without immediate recovery after force release. *Adhesiveness* refers to the force needed to separate two components, be they molecules, cell processes, or a cell process attached to an extracellular substrate. Recent methodological advances have enabled probing of mechanical/material properties with high resolution and sensitivity at molecular, cellular, and tissue levels [41–44].

2.3. Subcellular specializations for morphogenesis

Living cells have numerous specialized subregions that mediate their

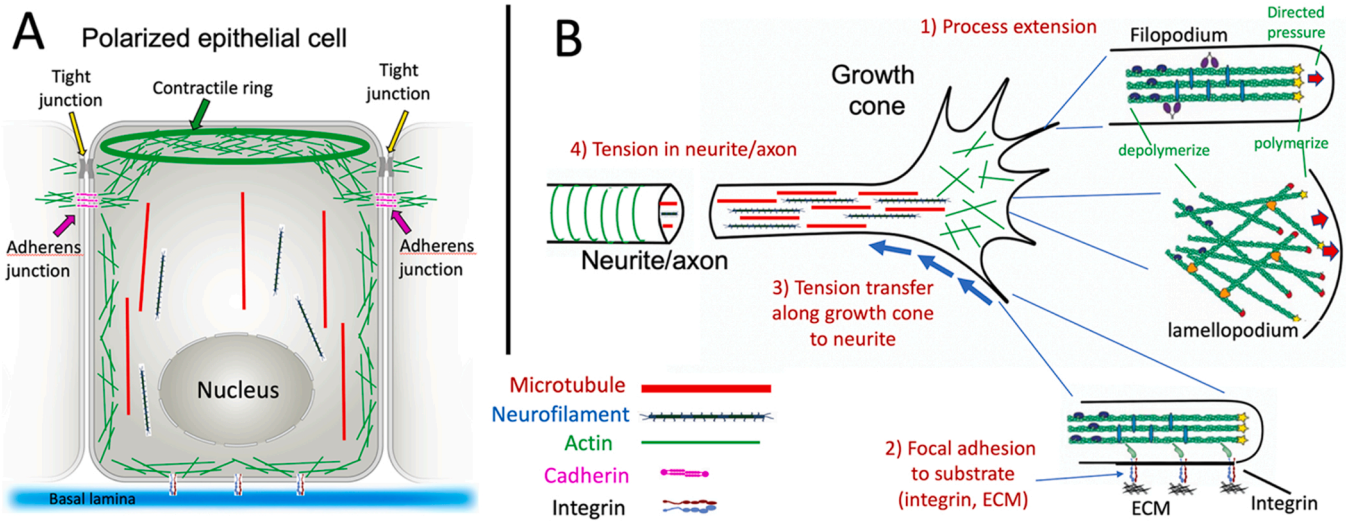

Fig. 1. Subcellular specializations for morphogenesis. A. Schematic polarized epithelial cell showing apical-basal polarization of tight junctions, cadherin-based adherens junctions, and actin meshwork. B. Key events and cellular components in a growth cone and an associated neurite. These events may occur concurrently or in any sequence. Panel B adapted from Fig. 2, ref. [1].

different functions. Among the subcellular specializations involved in morphogenesis, three warrant brief description here: *polarized epithelial cell domains*, *growth cones*, and *elongated processes* (*axons, dendrites, and neurites*) that dynamically regulate their length.

Polarized epithelial cell domains are established early in embryogenesis and include apical, basal, and lateral domains that differ in cytoskeletal organization and membrane constituents (Fig. 1A). The tight junctions between cells that form a diffusion barrier across the epithelial sheet are located near the apical surface. Immediately below, cadherin-based adherens junctions are linked to F-actin filaments that are continuous with the aforementioned actomyosin cortical meshwork. In some epithelial cells (and at some developmental stages), a cable-like actomyosin contractile ring encircles the apical perimeter.

Growth cones are specialized appendages that play critical roles in cell migration and in neurite/axonal/dendritic elongation and navigation (Fig. 1B). A growth cone typically has a central core with flat lamellopodial and/or spike-like filopodial extensions on one side and a trailing process on the opposite side. Actin polymerization generates directed pressure (red arrows in Fig. 1B) from crosslinked actin filaments that are colinear in filopodia and a planar mesh in lamellopodia [22,45,46]. Adhesion of the growth cone tip to ECM molecules enables actomyosin-mediated traction to advance the growth cone [47,48] and transfer tension to the growth cone rear [45].

Neurons growing in vitro extend processes that are often not readily distinguished as *axons* or *dendrites* and instead are called *'neurites'*. Neurites commonly exhibit 3 key characteristics: *resting tension*, *retraction* on tension release, and elongation when pulled (*'towed growth'*). *Resting tension* has been demonstrated in vitro for many neuronal types and species and in vivo for invertebrate axons [49–51]. Tension magnitude varies widely [40] and is much lower in chick forebrain neurites (~15 pN) [52] than in chick dorsal root ganglion neurites (0.5 – 6 nN) [53] and even lower (7 – 9 pN) in mouse hippocampal neurites [130] but should nonetheless suffice to impact morphogenesis in highly compliant CNS tissue. Neurites can transfer tension from the growth cone and also generate tension along their length, perhaps by an actomyosin-based process likely involving circumferential F-actin rings [25,54,55]. When tension is relaxed, retraction commonly occurs [56], and microtubule assembly/disassembly may be implicated in switching between neurite elongation and retraction [52,57]. *Towed growth or stress-induced elongation* can increase neurite or axonal length dramatically while maintaining diameter [58,59], likely involving pushing from microtubule sliding [60,61] but also involving neurofilament elongation

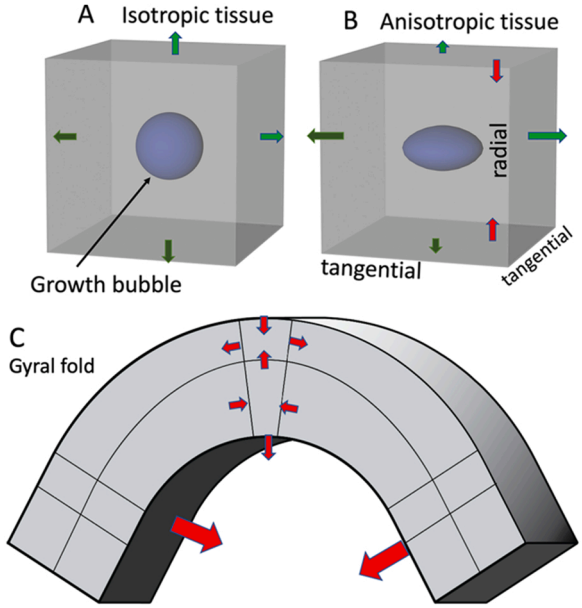

Fig. 2. Growth forces for soft tissue deformation. A. Spherical growth bubble and isotropic expansion (green arrows) in a cubical tissue 'voxel' with isotropic compliance. B. Oblate spheroidal growth bubble in a voxel with radially biased tension (red arrows) and hence anisotropic compliance and expansion. C. Laminar pattern of forces and deformations in a gyral region associated with folding forces.
Panels A, B Adapted from ref. [1].

[23]. This is relevant to models of cortical expansion discussed below.

2.4. Biomechanics of tissue morphogenesis

Given the forces and mechanical properties summarized above, an important general question is how to predict the tissue shape changes resulting from cellular growth and migration. Consider a microscopic (but multicellular) 'volume element' from a hypothetical embryonic CNS – a cubical 'voxel' containing various cell bodies and subcellular specializations. Suppose, for example, that a filopodial growth cone enters the voxel, increasing its volume by a tiny amount. The immediate

effects on voxel dimensions depend on the tissue's material properties – specifically, its compliance along each axis (Table 1B; see also Figs. 1.5 and 12.1 in ref [62]). If the compliance is isotropic (e.g., because the elongated processes in the voxel are randomly oriented and under resting tension) and if no additional forces arise from external sources, the incremental tissue expansion will be isotropic, represented by a spherical 'growth bubble' and equal-sized green expansion arrows (Fig. 2A). Moreover, a growth cone entering from the bottom, side, or top would cause the same isotropic expansion. In contrast, consider a voxel from a different region in which tissue compliance is anisotropic owing to radially biased cellular processes under tension (Fig. 2B, red arrows), but again with no additional external forces. In this case, tissue expansion will be anisotropic – illustrated by an ellipsoidal growth bubble (of equal volume) and unequal green arrows (Fig. 2B) that promote tangential expansion. A third example involves complex deformations spanning a larger domain, namely intracortical compressive, tensile, and shearing forces within a small cortical slab in the process of folding along one axis. As discussed below, such folding might occur in response to external forces such as axonal tension in the white matter (WM) that are transmitted via compliant but incompressible tissue into the interior of the slab (analogous to how a rubber pad folds in response to external bending forces). These forces can propagate through the tissue and lead to anisotropic forces having a predictable pattern along the axis of folding (red arrows at the gyral crown), where they compress from the side in deep cortical layers to make voxels taller and narrower but pull from the side in superficial layers to make voxels shorter and wider, resulting in progressive divergence of the radial axes near the crown (Fig. 2C).

Failure to appreciate such biomechanical fundamentals can lead to flawed hypotheses about possible mechanisms of morphogenesis. For example, the assertion that growing axons 'push' tissue ahead to form a gyrus, as suggested in ref. [63], would make sense only if axonal filopodia encountered tissue that was physically rigid (like a block of ice) rather than highly compliant. Neurons migrating into the cortical plate do not overtly 'push cells to the side' as suggested in ref. [64]. Instead, each cell should respond to the arrival of another cell in its vicinity by repositioning according to local forces and tissue compliance. Such tissue expansion patterns should be independent of the direction of cellular migration or ingrowth. More generally, when considering such issues, it is important to be mindful of standard biomechanical models of tissue growth kinematics based on material properties and forces [62,65].

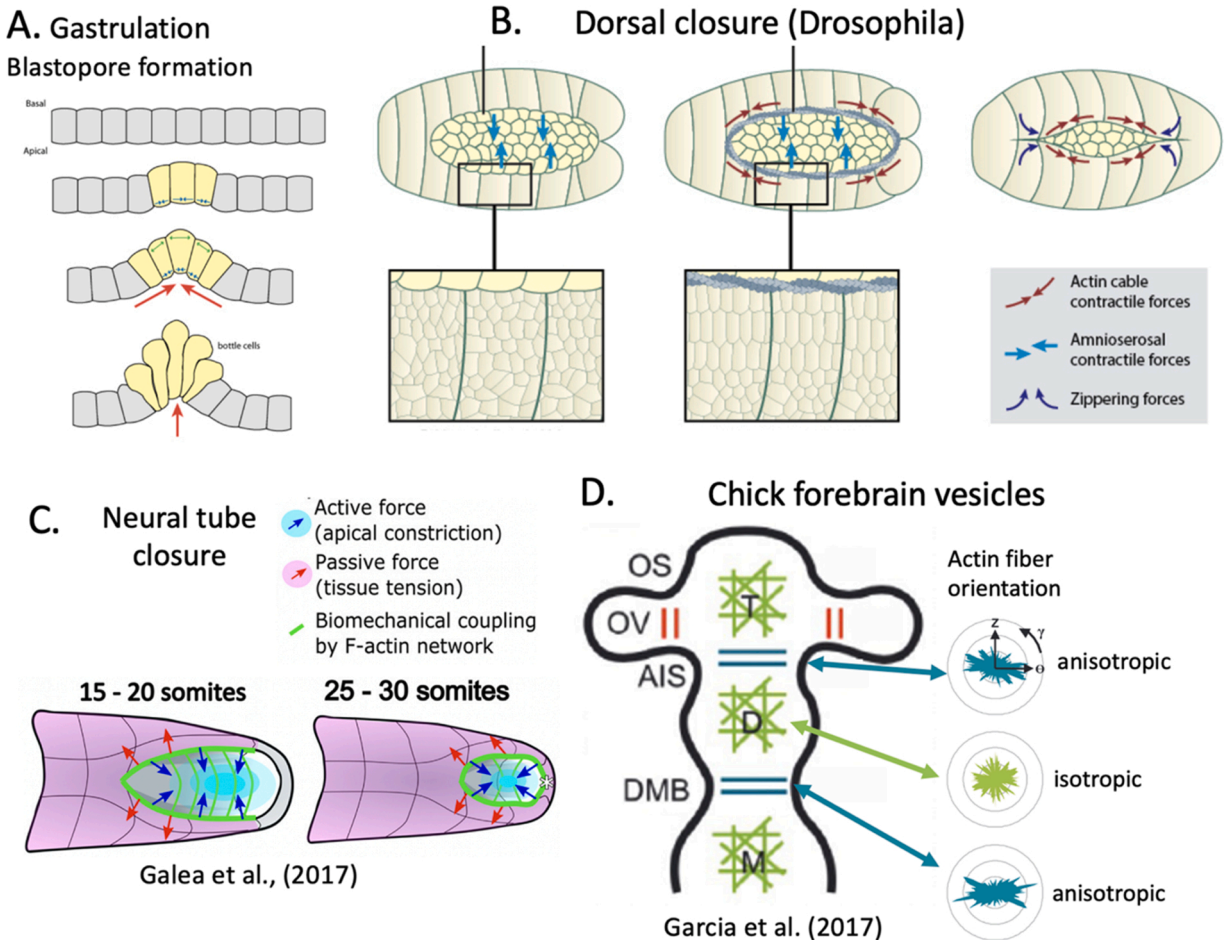

Fig. 3. Tension-generating events in early embryogenesis. A. Actomyosin-mediated apical constriction in bottle cells leads to invagination and blastopore formation. B. Dorsal closure in Drosophila includes contraction of an F-actin cable, amnioseral medio-lateral apical contraction, and zippering forces. C. Progressive closure of the neural tube by actomyosin-mediated zipping along the dorsal midline of the neural fold. D. In the developing chick forebrain, F-actin is oriented isotropically within the diencephalon (D), midbrain (M), and telencephalon (T) but has a circumferentially anisotropic orientation at the diencephalic-midbrain boundary (DMB) and along the anterior intraencephalic sulcus (AIS) at the diencephalic/telencephalic boundary. Contraction of these actomyosin rings likely contributes to brain vesicle formation.

A. Reproduced from https://commons.wikimedia.org/wiki/File:Apicalconstriction_fig1.jpg. B. Adapted from https://www.mechanobio.info/development/what-is-dorsal-closure/how-is-dorsal-closure-controlled-by-mechanics/ licensed under a Creative Commons Attribution-NonCommercial 4.0 International License. C. Adapted from Fig. 7 C of ref. [72]. D. Adapted with permission from Fig. 3, ref. [73].

2.5. Tension in early embryogenesis – from gastrulation to brain vesicles

The relative simplicity and accessibility of embryonic tissue has enabled numerous studies of mechanical forces in early embryogenesis. Fig. 3 schematically illustrates four developmental events in which tension is implicated as a major morphogenetic force: gastrulation in both invertebrate and vertebrate species, dorsal closure in Drosophila, neural tube formation in chordates, and embryonic brain vesicle formation in vertebrates. All four invoke actomyosin-based tension, and two of them invoke a process of tension-based 'zipping'.

A key early event in *gastrulation* is the invagination of surface ectodermal cells through the blastopore. A common feature involves apical constriction of ectodermal cells mediated by multiple types of actin-based or actomyosin-based contraction [66,67]. Fig. 3A schematizes the apical constriction process in so-called 'bottle' cells as they deform from a cylindrical to a flask shape.

Dorsal closure in Drosophila embryogenesis involves an elliptical zone in the epidermal layer that is initially covered by the amnioserosa, a squamous epithelium that does not contribute to the larva [68]. Dorsal closure involves several distinct steps in which forces mediated by F-actin and nonmuscle myosin II are implicated [69]: (i) Constriction of the apical region of amnioserosal cells shrinks their surface area and draws epidermal margins closer to one another (blue arrows, Fig. 3B). (ii) Contraction of an F-actin cable in cells along the epidermal margin acts as a 'purse string' to further shrink the gap (red arrows, Fig. 3B). (iii) Filopodia extend from leading-edge epidermal cells on either side and meet at the midline, then pull so as to zip the leading-edge epidermal cells together [71].

In chordates, *neurulation* begins with formation of the neural plate and neural groove along the dorsal midline. One component of this process involves contraction of medio-laterally oriented actomyosin cables, which drives apical constriction, makes cells wedge-shaped and elongated along the antero-posterior axis and promotes formation of a midline groove [74]. Closure of the neural groove to form a neural tube involves actin-rich filopodia and/or lamellopodia that are extended by neural ectoderm and/or non-neural ectoderm cells (depending on region, species, and stage). These processes meet at the midline and drive a zipping process [72,75,76] analogous to that just described for Drosophila dorsal closure.

Embryonic brain vesicles. Early vertebrate brain development includes the emergence of hindbrain, midbrain, and forebrain 'vesicles' followed by splitting of hindbrain and forebrain into additional vesicles. In chick embryos, elevated embryonic CSF (eCSF) pressure expands the initially quasi-cylindrical brain tube [77,78]. Contraction of circumferential actomyosin rings at presumptive vesicle boundaries (Fig. 3D) then appears to initiate conversion of the brain tube into the three primary vesicles [79] as well as further subdivision of the forebrain into telencephalic, diencephalic, and optic vesicles [73,79]. The expansion and stretching of the thin vesicle walls by elevated pressure may promote stress-dependent cell division [73,80], thereby enhancing the pace of expansion.

The examples covered in this section illustrate that mechanical tension mediated largely by actomyosin-based mechanisms are implicated in many early morphogenetic events and across diverse metazoan species. Many of the same biomechanical principles and mechanisms underlying these events in relatively simple embryonic systems are likely also to be engaged in anatomically more complex systems, such as the mammalian cerebral cortex that we turn to next.

3. Cerebral cortical growth and gyrification – an integrated biomechanical perspective

Cerebral cortex varies dramatically across mammalian species in terms of its overall size and the complexity of its convolutions. Many

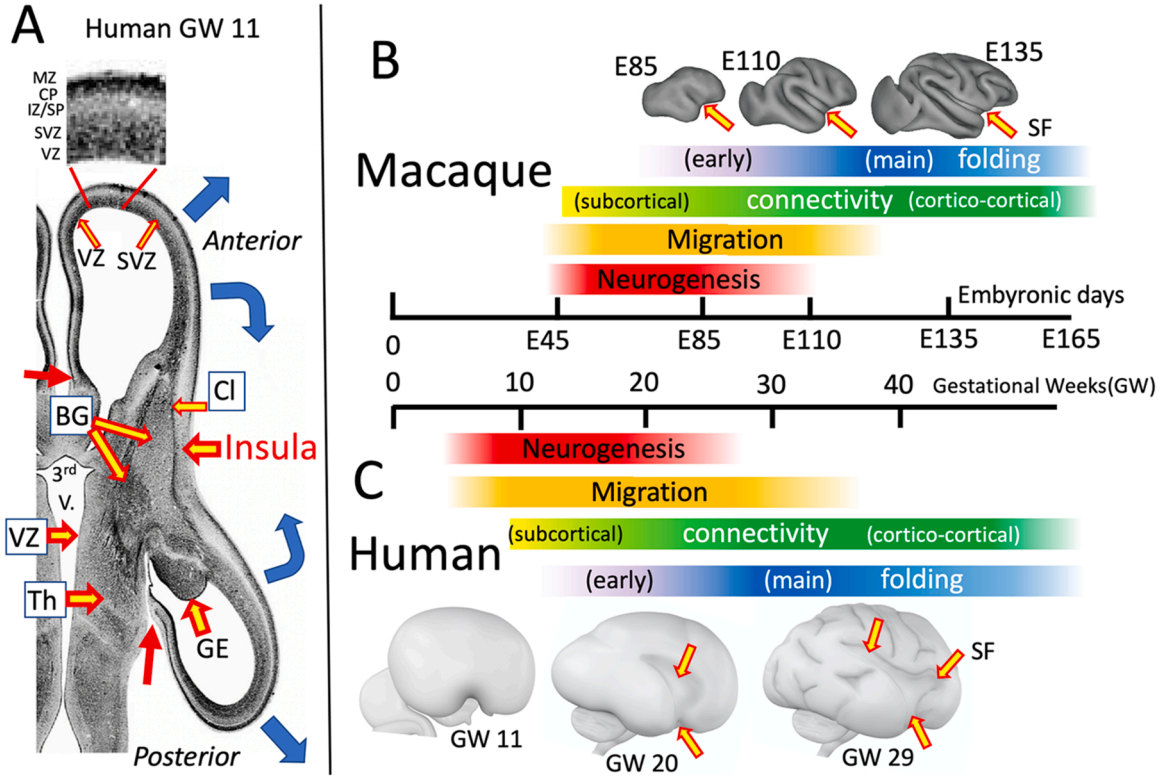

Fig. 4. Key events in primate cortical development. A. Horizontal section from human GW11 brain. Cl: claustrum. Other abbreviations as in main text. Blue arrows: cortical expansion trajectories; red arrows: junction between cerebral cortex and subcortical 'medial wall'. B, C. Timing of major events in macaque (B) and human (C) cortical development and folding [94,97]. SF: Sylvian Fissure. Macaque surface models are reprinted from ref. [131] , which is licensed under CC BY 4.0.
A. Republished with permission of Taylor & Francis Group LLC – Books, adapted with permission from ref. [82]; permission conveyed through Copyright Clearance Center. B, C Figure adapted from Fig. 4 of ref. [1].

developmental studies and reviews have focused specifically on the issue of cortical folding per se and have paid little attention to corollary questions of what regulates cortical thickness and surface area. Allometric studies show that the degree of cortical folding can be accurately predicted knowing just the total surface area and mean thickness [81]. It is important to consider all three issues (thickness, surface area, and folding) collectively in order to obtain an integrated mechanistic perspective.

3.1. Key events and stages in forebrain morphogenesis

Fig. 4A illustrates many important aspects of early brain development using a horizontal section through a gestational week (GW)11 human brain as an anatomical substrate [82]. Forebrain subcortical nuclei arise from a relatively thin ventricular germinal zone (VZ) of the diencephalon plus the thicker ganglionic eminence (GE) of the ventromedial telencephalon. Postmitotic neurons migrate relatively short distances to reach their final positions in specific nuclei and subnuclei of the thalamus, hypothalamus, and basal ganglia. The diencephalic vesicle collapses into the narrow third ventricle (3rd V.) lined by an increasingly thick gray matter wall. In the telencephalon, most of the lateral ventricle is bordered early on by a relatively thin cerebral wall that includes proliferative ventricular (VZ) and subventricular (SVZ) zones, a fibrous intermediate zone (IZ), a cortical subplate (SP) zone that contains scattered neurons and many synapses in their so-called 'waiting period' [83] as well as many axons and radial glial processes, a cell-dense cortical plate (CP), and a thin fibrous marginal zone (MZ) capped by a basal lamina. As noted above for the chick embryo, stretching of the thin cerebral wall from elevated CSF pressure may accelerate proliferation of neuronal precursors in the VZ and SVZ that populate the cerebral cortex.

Fig. 4 also shows timelines of major events during the development of cerebral cortex for the macaque (panel B) and human (panel C). Cortical neurogenesis (red bars) extends over a ~2 month period in the macaque [84,85] and more than 4 months in humans [86]. Neuronal migration (orange bars) starts near the onset of neurogenesis but extends even longer than does neurogenesis. Excitatory (pyramidal) neurons are born in the germinal (ventricular) and subventricular zones and migrate mainly radially along scaffolding formed by multiple subtypes of radial glial cell (RGC). These include ventricular RGCs (vRGCs) closest to the VZ plus outer RGCs (oRGCs) whose cell bodies are in the SVZ [87,88]. Alternative names for ventricular and outer RGCs are apical and basal RGCs (aRGC and bRGCs), respectively [9]. Later-born excitatory neurons originate from precursors in the SVZ, and their migration through the IZ/SP may involve jumping from one RGC to another with some tangential migration in between, as shown in ferret cortex [10]. On arrival at the CP, neurons migrate past deeper (earlier-born) cortical neurons and settle superficially, just below the MZ that later becomes layer 1 [89,90]. Inhibitory neurons are born in the GE and migrate long distances tangentially through the cortex to reach their termination. Long-distance connections through the WM are established over an even longer period (yellow/green bars) than cellular migration, starting first with connections to subcortical nuclei soon after deep-layer cortical neurons have arrived. Cortical synapse formation and WM expansion involving cortico-cortical and cortico-subcortical pathways occur throughout the third trimester [86] (green portion of connectivity bar). In the macaque (Fig. 4B), long-distance cortico-cortical connections reach the subplate and/or cortical plate beginning ~embryonic day (E) 106 for area V4 [91] and ~E108 for V1-V2 [92]. This overlaps with the main gyrification period (~E100 to ~E135) [93–95]. Axons tend to run in parallel in the developing WM, forming numerous long-distance fiber tracts. However, extensive crossing of fiber bundles must occur in order to achieve the brain's enormous wiring complexity (e.g., an average of >50 input and output pathways to each cortical area in the macaque [96]). Hence, WM wiring must have high topological complexity, which has important implications for aggregate wiring length as the brain grows (see ref. [1], SI Topic 6).

3.2. 'Early' cortical folding

In primates the main gyrification period is preceded by three distinct types of 'early' cortical folding (purple preceding blue in Figs. 4B and 4 C), two of which emerge as a result of unique types of differential neuronal proliferation. (i) *Sylvian Fissure (SF).* The primate insula arises early from a distant germinal region at the pallial-subpallial boundary [98] and is anchored by its strong connections with the adjacent slow-growing claustrum and basal ganglia (Fig. 4 A). Neighboring neocortical regions are not anchored but instead expand rapidly (blue arrows) in conjunction with the expanding lateral ventricles; the underlying germinal layers near the ventricular surface also expand. The SF begins as a crease along the perimeter of the insula (the nascent circular sulcus) starting before E85 in the macaque [94] and before GW20 in humans [97]; by E110 in the macaque and GW29 in humans the temporal, parietal, and frontal gyral regions approach one another to form a well-defined SF (top row in Fig. 4B, bottom row in Fig. 4 C). (ii) *Early calcarine sulcus.* In macaque occipital cortex, in utero MR scans at E85 (Fig. 5 A, top) and E90 (Fig. 5 A, lower left) reveal a nascent calcarine sulcus (CaS) appearing as a distinct indentation of the cortical

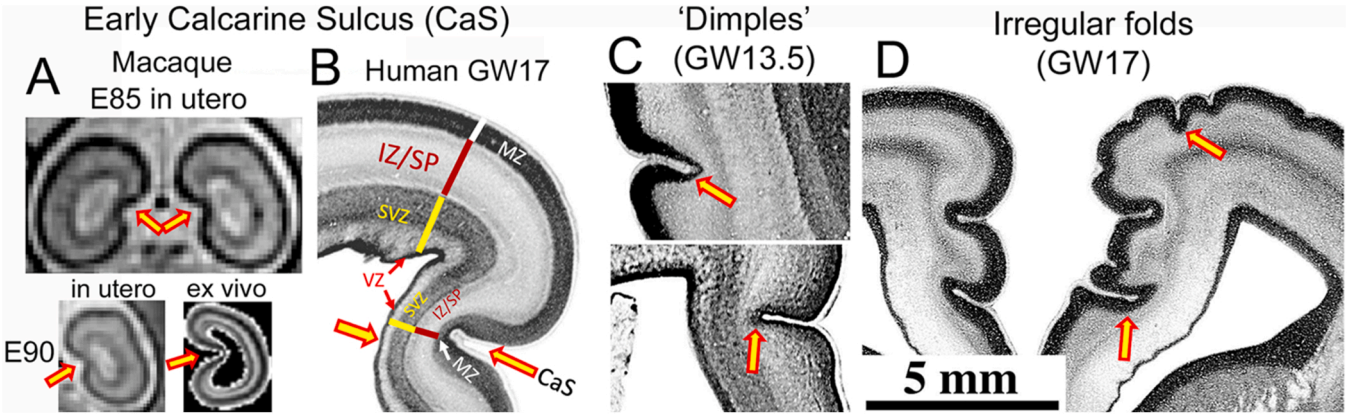

Fig. 5. Early-forming cortical sulci in primates. A. Macaque early calcarine sulcus at E85 in utero (top) and at E90 in utero (bottom left) and ex vivo (bottom right). B. Human early calcarine sulcus at GW17 (coronal). C. "Dimples" in lateral temporal (top) and medial frontal (bottom) cortex at GW13.5. D. Early irregular folds in frontal cortex at GW17.

A. Images adapted with permission from ref. [93]. D. Images in B – D adapted with permission from ref. [97]. Republished with permission of Taylor & Francis Group LLC – Books, from ref. [97]; permission conveyed through Copyright Clearance Center, Inc. Figure adapted from Fig. 5 of ref. [1].

plate and an IZ that is thin or absent. Given that the earliest V1-V2 connections reported are at E108 [92], formation of this early calcarine sulcus seems unlikely to be related to cortico-cortical connectivity. In an E90 ex vivo scan, the calcarine invagination is deeper, and a bulge into the posterior horn in the region corresponds to a feature known as the calcar avis in adults, but at this early age the inward bulge likely reflects a brain extraction or fixation artifact. In human postmortem histological sections, a precursor to the calcarine sulcus is discernible at GW13.5 – GW21 [83,97,99], including the GW17 example in Fig. 5B (arrows) where the proliferative zones (VZ, SVZ) plus the IZ and SP are much thinner than in adjacent regions. As in the macaque there is a pronounced invagination into the ventricle (wide arrow in Fig. 5B) that is not evident in in vivo human MRI scans prior to GW23–24 (ref. [100] and G. Kasprian, personal communication) and thus is likely an artifact of brain extraction and/or fixation. However, it is unlikely that the dramatic thinning of the cerebral wall is entirely artifactual; more likely, it largely reflects differential thickness and differential proliferation of the germinal layers. (iii) A very distinct type of early folding involves small dimples and wrinkles that appear early in the second trimester in human postmortem brain sections (Fig. 5 C, D). These are irregular in location, shape, and spacing [97,99] and many of them may be transient structures. These invaginations are typically most pronounced in superficial layers, suggesting they are initiated by superficial morphogenetic forces. Even if they ultimately prove to be fixation artifacts, they suggest a distinct type of mechanical instability in cortical tissue at this stage.

3.3. Models and mechanisms of cerebral cortical expansion and folding

Numerous models and mechanisms have been proposed to account for cortical expansion and folding, and others have noted the plausibility of contributions from multiple mechanisms [101]. Here, we focus on three major models, each of which invokes multiple mechanistic components. Two models have been previously published: the Radial Divergence (RD) model [9,10] and the Gel-Brain Bilayer (GBB) model [11]. The third is largely based on my recent Differential Expansion Sandwich Plus (DES+) model [1], but here it is refined in several respects. Also, it is renamed as the Composite Tension Plus (CT+) model to signify a prominent and multifaceted role for tension along with inclusion of other mechanisms, including several also invoked by the RD and

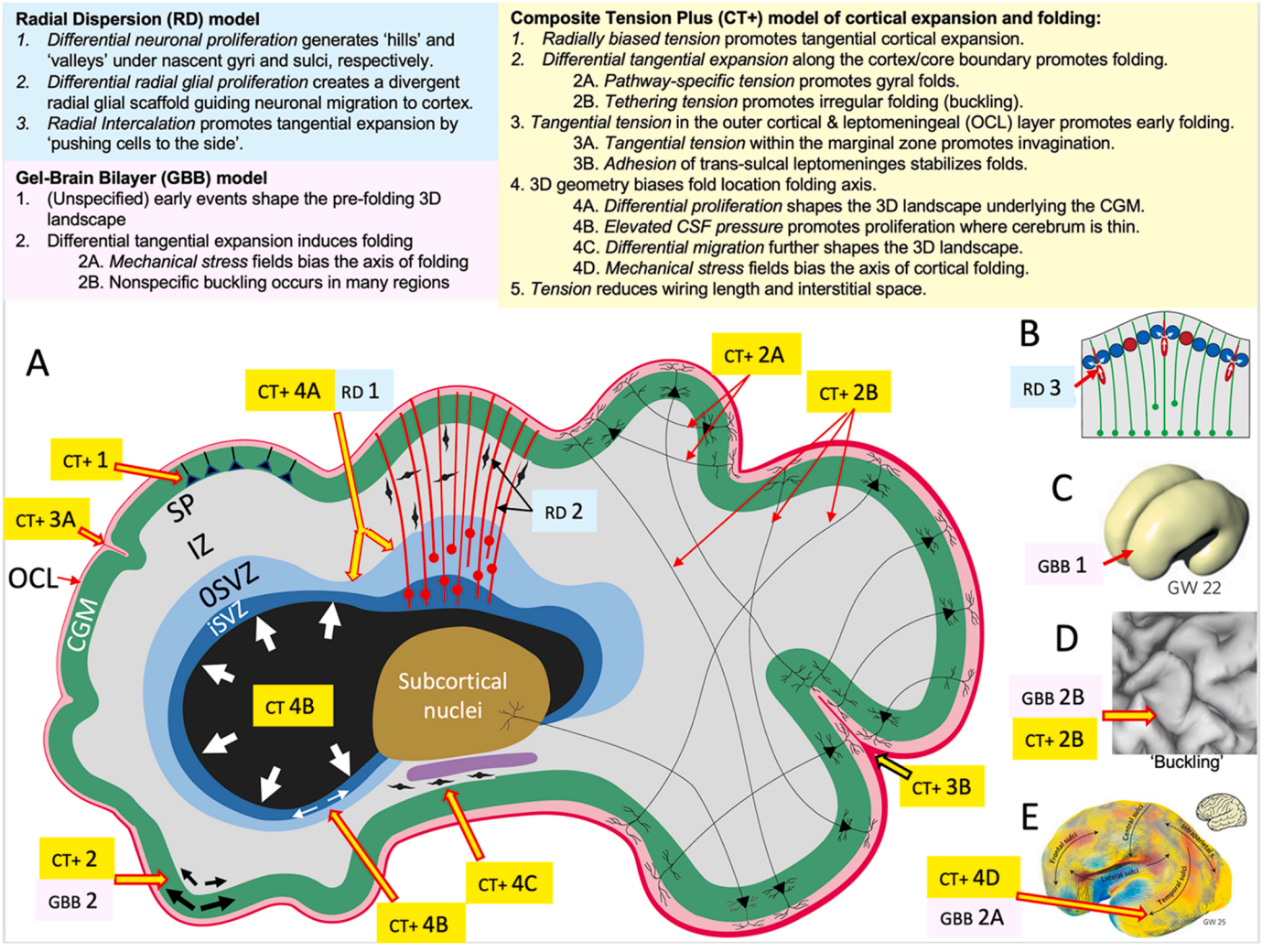

Fig. 6. Three models of cortical expansion and folding. Top left. Tenets of the RD (blue) and GBB (pink) models. Top right. Tenets and subtenets of the CT+ model (yellow). Bottom. A. Models of cortical expansion and folding displayed on a schematic illustration of key aspects of cortical development, with features prominent at earlier stages on the left and those prominent at later stages on the right. CT+ tenet 5 (compact wiring) is not denoted in panel A because it presumed to be mediated by all elongated processes that are under tension. B. Schematic of Radial Intercalation model. C. Computer 3D model of a human GW22 brain. D. Exemplar surface of a highly convoluted and irregularly folded region in human prefrontal cortex in individual HCP subject 100307. E. Strain fields in computerized version of GBB model that bias fold orientation.
B. Adapted with permission from ref. [64]. C. Adapted with permission from Fig. 1d of ref [11]. E. Adapted with permission Fig. 3a of ref [11].

GBB models. Each model is described briefly in relation to Fig. 6, which schematically illustrates major mechanistic events and processes. All three models are then evaluated systematically with reference to Table 2, where each column refers to a proposed component mechanism for a given model, each row represents an experimental observation needing explanation, and each cell qualitatively indicates the explanatory capacity of that mechanism (column) for that observation (row). In both the figure and table, pastel shades associate various entries with one of the three models (blue for RD, pink for GBB, yellow for CT+).

The RD model (pastel blue text in Fig. 6 and columns b – d in Table 2) invokes three complementary mechanisms: *differential neuronal proliferation* (column b), *differential RGC proliferation and divergence* (column c), and *radial intercalation* of neurons into cortical gray matter (CGM, column d). (i) *Differential neuronal proliferation* posits that genetically regulated fluctuations in the thickness of the underlying germinal zones, particularly the SVZ ('RD 1' in Fig. 6 A) give rise to 'hills' and 'valleys' in the 3D landscape and that the numbers of neurons produced under nascent gyri and sulci correlate with germinal zone thickness. (ii) *Differential RGC proliferation and divergence* posits a corresponding differential production of bRGCs under nascent gyri vs sulci, in the inner and outer SVZ (iSVZ, oSVZ), leading to divergence (fanning out) of gyral but not sulcal radial glial basal processes in the IZ and SP ('RD 2' in Fig. 6 A). It also posits that the migration of pyramidal neuron precursors often includes a tangential component (jumping from one radial glial process to another) along with predominantly radial migration [9,10]. (iii) As migrating neurons reach their target layer at the top of the CP, a *radial intercalation* mechanism [64] posits that newly arrived neurons overtly push neighboring cells 'to the side' and thereby promote tangential cortical expansion ('RD 3' in Fig. 6B).

For differential tangential expansion (DTE) models, the core notion is that when adjacent 'layers' expand tangentially at different rates, instabilities and/or biased forces along their common interface promote cortical folding. The Gel-Brain Bilayer (GBB) model [11] is a specific instance of a DTE model that involves two main stages (pink in Fig. 6 and Table 2). Stage 1 takes as a given an initial 3D configuration that matches the smooth but complex shape of the brain in an early (GW22) human fetal brain (GBB 1 in Fig. 6 C). This shape is presumed to reflect the myriad factors needed to generate a minimally folded brain, such as the differential proliferative mechanisms invoked by the RD model described above, but these are not explicitly specified in the GBB model. The physical GBB model was made by creating an elastomer inner core molded to match GW22 brain shape, which was coated with a thin, softer outer elastomer layer representing the initial thickness of the CGM. Immersion in a solvent (and running an equivalent computer simulation) caused the outer layer to expand faster than the inner layer (GBB 2 in Fig. 6 A), resulting in folding that strikingly recapitulates observed patterns of human cortical folding. This includes some primary folds aligned to overall lobar shape owing to nonlinear instabilities operating on mechanical stress fields arising from the initial 3D brain shape (GBB 2 A in Fig. 6E) as well as quasi-random buckling in other regions (GBB 2B, Fig. 6D).

The Composite Tension Plus (CT+) model (pastel yellow entries) is expressed as 5 tenets and multiple sub-tenets. *Tenet 1. Radially biased tension* in elongated processes anchored within the CGM promotes tangential cortical expansion (CT+ 1 in Fig. 6 A). *Tenet 2. Differential tangential expansion* along the cortex/core boundary (CT+ 2 in Fig. 6 A) promotes folding in two complementary ways: *Tenet 2 A. Pathway-specific tension* promotes gyral folds by bringing strongly connected nearby cortical areas closer together, forming a gyrus in between (CT+ 2 A in Fig. 6 A); *Tenet 2B. Tethering tension* promotes irregular folding (buckling) along the cortex/core boundary (CT+ 2B in Fig. 6 A). The distinction between tethering and pathway-specific tension is not an all-or-nothing dichotomy; many axons likely contribute to both processes. *Tenet 3. Tangential tension* along the outer cortical and leptomeningeal (OCL) layer plus trans-sulcal pial adhesion promote early folding. *Tenet 3 A. Tangential tension* within the marginal zone (later, layer 1) has a

Table 2
Explanatory power of cortical expansion and folding models and mechanisms.

	MODEL:		RADIAL DIVERGENCE (RD)			GEL-BRAIN BILAYER (GBB)			COMPOSITE TENSION PLUS (CT+)									
	Tenet (CT+ model only):						DTE		T1: RBT	T2: DTE		T3: OCT		T4: 3D Geometry				T5: CW
a	b	c	d	e	f	g	h	i	j	k	l	m	n	o	p	q	r	s
	Mechanism (CT+ tenet/subtenet) OBSERVATION (Experimental finding)	REF	Differential neuronal proliferation	Differential RGC proliferation, divergence	Radial intercalation	GBB 1: Early 3D geometry	GBB 2A: Stress fields bias folding axis	GBB 2B: Quasi-random buckling	T1: Radially biased tension	T2A: Pathway -specific tension	T2B: Tethering tension	T3A: Marginal zone puckering	T3B: Lepto-meningeal adhesion	T4A: Differential proliferation (neurons, radial glia)	T4B: Germinal layer stretching induces proliferation	T4C: Differential migration	T4D: Stress fields bias folding axis	T5: Tension makes wiring compact
1	Preferential tangential expansion	82 97			X[62]				+[93]						+[73]			
2	Thickness varies with age, area	102 103			X[62]				+[93,94]									
3	Tangential CGM cuts: no gap	12							X[1,106]									
4	Folding-proliferation correlation (partial)	10 108	+[107]											+[109]				
5	Divergent radial trajectories (gyri)	10		+[10]										+		+		
6	Folding without cranial pressure	110	+	+			+	+	+	+	+							+
7	Low interstitial space; core is 'shrink-wrapped'	97 108 111							+	+	+							+
8	Connectivity-folding correlation	3 113 114	+							+								+
9	Areal boundaries partly correlated with folds	3 102 114	+							+	+							
10	Tissue cuts parallel to WM gyral blade: no gap	12								X[1,106]								
11	Macaque V1/V2: short paths, gyrus near border	117								+								+
12	Folding irregularity ('buckling')	118						+			+[12]	+[119]						
13	Tissue cuts in deep WM: gap	12 120									+							
14	Tissue cuts orthogonal to WM gyral blade: gap	12									+							
15	Folds aligned to lobes	118					+[11]										+[11]	
16	Trans-pial adherence	1										+[119]	+[119]					
17	Early irregular dimples, creases	97										+[12]	+[119]					
18	Folding-related architectonic distortions	121 122		+[10]			+[11]										+[11]	

Columns a - c: observation number, name, and associated reference. Columns d - s; 16 putative mechanisms grouped by model: – RD (blue), GBB (pink), and CT+ (yellow). Rows 1 – 18: experimental observations that support some mechanisms (green cells with '+'), are inconsistent with others (cells with 'X'), or are neutral. Superscripts indicate relevant references in columns c - s.

'puckering' effect that promotes invagination of the CGM (CT+ 3 A in Fig. 6 A). *Tenet 3B. Adhesion* of the leptomeninges (pial basal lamina plus ECM) across apposed banks of a sulcus tend to stabilize folds by allowing them to slide relative to one another while remaining physically adherent (CT+ 3B in Fig. 6 A). *Tenet 4. Three-dimensional geometry* biases the location of folds and the axis of folding. *Tenet 4 A. Differential proliferation* shapes the 3D landscape by regulating the number of neurons and radial glial cells generated in major proliferative zones (VZ, iSVZ, oSVZ) and by regulating the thickness and ventricular surface area associated with different regions (CT+ 4 A in Fig. 6 A). *Tenet 4B. Elevated CSF pressure* stretches the germinal zone, particularly in regions where it is thin, which can lead to stretch-induced proliferation and further ventricular enlargement, particularly in highly gyrencephalic species (CT+ 4B in Fig. 6 A). *Tenet 4 C. Differential migration* further shapes the 3D landscape by regulating the predominantly radial migration of excitatory neuron precursors and the predominantly tangential migration of inhibitory neuron precursors (CT+ 4 C in Fig. 6 A). Tenet 4D. *The axis of cortical folding* may be biased by mechanical stress fields that are related to the overall 3D configuration of the developing brain (CT+ 4D in Fig. 6E). Tenet 5: *Tension reduces wiring length and interstitial space*, thereby ensuring that the developing brain does not expand to loosely fill all available space.

3.4. Evaluation of the three models

To facilitate systematic within-model evaluations and cross-model comparisons, Table 2 lists 18 experimental observations that are directly or indirectly informative about mechanical factors and forces that may impact cortical expansion and folding and help elucidate the explanatory power and limitations of different models and mechanisms. These include characteristics reported during normal cortical morphogenesis and findings from experimental perturbations. Column 'b' states the observation succinctly, and column 'c' provides key reference(s) that document the observation. Each cell at the intersection of a given row and column contains a '+ ' and is colored green if the mechanism associated with that column qualitatively accounts for the observation associated with that row or at least could plausibly be a major contributing factor. If the observation is inconsistent with the mechanism, the cell instead contains an 'X' and is red if the inconsistency is severe or orange if there are plausible alternative explanations for the inconsistency. The majority of cells are blank (with a pastel color matching the model type) because the observation for that row is neutral with regard to the mechanism associated with that column. References listed in individual cells provide key additional evidence pertaining to how well that mechanism does or does not account for the observation.

The first two observations pertain to the cortical sheet independent of whether it is folded: (1) cortical expansion is preferentially tangential [82,97] and (2) cortical thickness varies systematically with developmental age and across cortical areas [102,103]. The radial intercalation mechanism invoked by the RD model proposes that neurons overtly push neighboring cells 'to the side' in order to promote tangential cortical expansion and keep the cortex thin. However, radial intercalation is not a biomechanically plausible mechanism for expansion of soft, pliable CNS tissue in general ([62]; see also Section 1.4 and Fig. 1A, B). Hence cells '1 f' and '2 f' in Table 2 are red and contain an 'X' because radial intercalation does not account for tangential expansion or thickness. Unless radial intercalation is supplanted by a viable alternative mechanism (e.g., radially biased tension within the CGM), the RD model as currently formulated [9,104,105] would allow neurons migrating into the cortical plate to stack up radially and make CGM thicker and smaller in surface area. The GBB model does not account for preferential tangential expansion or changes in cortical thickness because in the physical model, thickness was not measured and in the simulation these characteristics were imposed by explicit growth equations rather than emerging independently [11].

In contrast, the CT+ model accounts for both preferential tangential expansion and cortical thickness that varies with age and across areas based on the degree of radial bias in tension-bearing elongated fibers within CGM (Tenet 1), given that the radial bias changes with age [93] and can vary across cortical regions [94]. Also, elevated ventricular CSF pressure stretches the cerebral wall in regions where it is thin to begin with and can accelerate neuronal proliferation [73]. Accordingly, cells 1j, 1p, and 2j in Table 2 are green and contain a '+ '. To my knowledge, these are the only proposed mechanisms that can account for either observation 1 or 2. However, observation 3 is that tangential tissue cuts in CGM of *ex vivo* brain slices of ferrets failed to show a gap indicative of resting radial tension [12], contrary to the prediction of CT+ Tenet 1. Importantly, the tissue-cut paradigm might cause osmotic shock and metabolic stress in tissue slices, thereby obscuring resting tension that could be present in vivo (ref. [106]; see [1] for details). Accordingly, cell 3j (Table 2) has an 'X' to indicate inconsistency but is shaded orange rather than red in order to reflect this viable alternative explanation. Moreover, even if radial tension were shown to be lacking in ferret CGM in vivo, the conclusion would not necessarily generalize to other species, especially given the many known differences in cortical development in primates vs ferrets. While it is conceivable that regulation of cortical thickness and tangential expansion are mediated by novel mechanism (s), a parsimonious alternative is that radial tension indeed plays a prominent role despite imperfect evidence to the contrary from a single experimental study.

Observation 4 is that folding patterns correlate with differential proliferation, as predicted in general by the RD model (cell 4c, Table 2) and for some regions in some species by the CT+ model (cell 4o). The strongest evidence for a correlation comes from ferret visual cortex, where thicker vs thinner underlying proliferative zones (especially the oSVZ) respectively underly nascent gyri and sulci and also correlate with neuronal proliferation rates [10]. In humans and nonhuman primates, evidence for folding correlated with differential proliferation has already been noted for the special cases of the SF and the calcarine sulcus (Section 3.2). Differential proliferation may contribute to the formation of other primary sulci in human and macaque, as has been proposed [107] but also challenged. If differential proliferation were the main determinant of the precise and complete folding pattern in highly gyrencephalic species, the 3D landscape of hills and valleys in the germinal zones would need to be highly corrugated, mirroring the corresponding cortical convolutions in the adult. Such a pattern is not evident during the second and third trimesters of human development [97,108,109]. Thus, there are likely to be major species differences in the degree to which differential proliferation contributes to folding.

Observation 5 is that radial glial trajectories diverge under nascent gyri owing to differential proliferation of basal RGCs, as shown most clearly in ferret visual cortex [10]. This can be explained by RD mechanism 5e and CT+ mechanisms 5o and 5q in Table 2 (Tenets 4 A, 4 C). Quantitatively, the degree to which this mechanism contributes to folding in different species remains to be determined. A corollary observation is that many radially migrating neuronal precursors also have a tangential component that involves exiting one RGC, migrating some distance tangentially, and attaching to another RGC process to continue their radial journey [10]. Such divergent tangential migration presumably leads to dispersion and intermixing of neurons originating from different initial radial glial columns, but it seems unlikely to impact the folding process per se because it would not impact the number of neurons entering a given gyrus or sulcus.

Observation 6 is that relatively normal cortical folding occurs even after removal of cranial pressure by brain size reduction via surgical removal of the opposite hemisphere [110]. Folding in the absence of cranial pressure is consistent with the differential neuronal and radial glial proliferation mechanisms of the RD model (cells 6d,e) and CT+ model (cell 6o), the DTE mechanisms of the GBB model (cells 6 h,i) and CT+ model (cells 6j,k,l), and the CT+ compact wiring mechanism (cell 6 s). Observation 7 is that interstitial space is generally low in developing brain tissue (i.e., outside the ventricles), even in the vicinity

of cortical folds as they are forming, based on histological sections [97] as well as in vivo prenatal MRI scans [111]. To appreciate the relevance of these two observations, consider a hypothetical variant of the GBB model in which adhesion between the two elastomer layers is completely lacking. In that situation, as the outer layer expands rapidly it could physically separate and drift away from the slowly expanding inner core. This could result in two separate layers, each expanded but with few if any convolutions in either layer. In the real brain, the physical continuity of axons entering and leaving the CGM prevent a complete separation between CGM and the WM core. However, an approximation to this hypothetical situation could arise if axons crossing the CGM/WM boundary elongated by towed growth (see Section 1.3) to an arbitrary degree when put under the slightest tensile stress – much as a fishing line can freely extend until the bail is engaged. This scenario has indeed been explicitly proposed [112]: "This suggests that - rather than axons pulling on the brain to induce cortical folding - the folding cortex pulls on the axons to trigger axonal elongation and white matter growth". However, unconstrained axonal elongation model could lead to a smoother CGM and a WM core having lower axonal density and excess interstitial space (and perhaps even CSF-filled cavities). In the CT+ model this hypothetical scenario is avoided and observation 7 is accounted for in part by tension-related mechanisms, including cells 7j, k,l plus cell 7 s, which posits that tension reduces both interstitial space and also aggregate wiring length (CT+ Tenet 5).

The next two observations are that (8) gyral folds often occur between strongly connected regions and that (9) some areal boundaries run close to gyral crowns or sulcal fundi. These relationships are best documented in the macaque [3,113,114]. In general, inter-areal connections tend to be strongest between nearby areas, and on average connectivity declines exponentially with distance between areas via white matter [115]. Both the RD and CT+ models can account for these observations, but for different reasons. In the RD model folding-connectivity and folding-areal boundary correlations (cells 8d, 9d) are secondary to the correlation between areal boundaries (near a gyral crown) and local proliferation maxima (cell 4c). The CT+ model instead accounts directly for folding-connectivity correlations through Tenet 2 A (pathway-specific tension, cell 8k) and indirectly for area-folding correlations (cell 9k in Table 2) as a corollary of the same process. The fact that many human areal boundaries are not closely correlated with gyral folds [102] is consistent with buckling-like folding posited by tethering tension (cell 8 l). The GBB model does not account for either observation 8 or 9.

Another key observation (10) is that tissue cuts in white matter parallel to a gyral blade in immature ferrets failed to show a convincing gap indicative of resting tension in the white matter between neighboring sulcal banks [12]. The RD and GBB models are neutral regarding this observation, whereas Tenet 2 A (pathway-specific tension) of the CT+ model predicts that tension should be observed and is thus inconsistent with observation 10 ('X' in cell 10k). However, the same reasons detailed above (observation 3) for suspecting an artifact in the ex vivo CGM tissue-cut experiment apply to observation 10, and cell 10k is accordingly colored orange. Moreover, even if future studies definitively establish that tension is indeed lacking in short-range cross-sulcal connections in vivo in the ferret, such a finding would not necessarily generalize to primates, where the geometry is very different and mechanisms related to proliferation and migration may be less pronounced. Observation 11 addresses this by considering the extreme example of areas V1 and V2, the two largest cortical areas in primates, each of which contains a precise retinotopic map. In the macaque, a high percentage of V1 neurons project to retinotopically corresponding parts of V2 and vice-versa, and the trajectories of the V1-V2 pathway are near-minimal in length throughout [117]. This is because a gyral fold runs along the V1/V2 border for its entire extent (bordering the lunate and inferior occipital sulci and both banks of the calcarine sulcus), bringing corresponding V1 and V2 sites into close proximity. This is readily explained in terms of pathway-specific tension (cell 11k) and compact wiring (cell 11 s) but not by RD or GBB mechanisms.

Observation 12 is that folding in many regions is highly irregular and variable across individuals, particularly for tertiary folds in human cortex [118]. The RD model as proposed does not explicitly account for this observation. Moreover, variability is greatest for tertiary folds, where the evidence of a correlated pattern of differential proliferation is weakest. The GBB model accounts for buckling-like irregularities by invoking instabilities caused by differential expansion along the CGM/WM border (cell 12i). The CT+ model also invokes local instabilities along the gray-white border, but attributes them to tethering tension between cortex and distant subcortical and cortical targets (cell 12 l), enhanced by puckering at quasi-random locations initiated by tangential tension in the OCL[119] (cell 12 m). The distinction between tethering and pathway-specific tension is not an all-or-nothing dichotomy; many axons likely contribute to both processes. Observations 13 and 14 are that gaps indicative of resting tension occur for tissue cuts in deep white matter of ferrets and mice and for cuts orthogonal to WM blades under a gyrus in ferrets [12,120]. The RD and GBB models are neutral with regard to these observations, whereas they both fit the predictions of Tenet 2B of the CT+ model (cells 13k, 14k), i.e., they provide positive evidence for the presence of tethering tension.

Observation 15 is that some folds are aligned with the long axis of cortical lobes, such as the superior temporal sulcus (STS) and nearby gyri and sulci in both macaques and humans (Fig. 6E). The RD model does not explicitly address this observation. The GBB model accounts for folds aligned to overall lobar shape by invoking nonlinear instabilities operating on mechanical stress fields arising from the initial 3D brain shape [11], as does the CT+ model for the same reason (cells 15 h,15r).

Observation 16 is that apposed banks of sulci often and at all ages are contiguous with one another along the pia mater, indicative of trans-pial adherence (ref. [1], SI Topic 4). This is not addressed by the RD or GBB models, but is accounted for by Tenet 3B (cell 16 n) involving trans-sulcal pial adhesion [119]. Observation 17 is that irregular dimples and creases are common in postmortem human histological sections prior to the main phase of major cortico-cortical connections [97], and they commonly have an atypical architecture involving greater invagination of superficial vs deep cortical layers (Fig. 5C, D). Neither the RD nor the GBB model accounts for these early cortical sulci. The CT+ model accounts for these features by invoking tangential tension and trans-pial adherence along the outer cortical and leptomeningeal (OCL) layer [12,119] (Tenets 3 A,B, cells 17 m,n). The OCL has previously received little attention as a source of morphogenetic forces but is currently the only proposed mechanism that can account for these early cortical folds.

Observation 18 is that cortical folding involves systematic architectonic deformations of laminar and radial organization and of cell morphology [105,121,122] (see Fig. 1). In gyral crowns, radial axes diverge from the base; deep layers are thicker and have tall, narrow dendritic arbors vs. short, wide arbors in thinner superficial layers. In sulcal fundi, the pattern is reversed. This observation can be partially explained by radial glial divergence in the RD model (cell 18d) and by the effects of mechanical stress fields in the GBB model [11] (cell 18 h) and the CT+ model (18r).

3.5. *Evaluation of three models - summary*

Several general observations and conclusions emerge from the analysis up to this point. In broad terms, it seems apparent that numerous morphogenetic mechanisms are likely to be engaged in cortical expansion and folding. The RD and GBB models in aggregate include five distinct mechanisms, but together they account for only 9 of the 18 observations. Of these 5 putative mechanisms, only the radial intercalation method is considered invalid, and that is for reasons related to biomechanical implausibility rather than experimental data. The CT+ model accounts for all but two observations; it achieves this breadth by bringing under one umbrella 10 mechanisms derived from

four sources: (i) mechanisms related to tension and pressure as presented in the original TBM hypothesis [3] (Tenets 1, 2, and 5); (ii) additional effects of tension plus adhesive forces in the OCL (Tenets 3 A, 3B) from the DES model [1]; (iii) contributions of differential proliferation and migration from the RD model [9,10]; and (iv) DTE mechanisms of the GBB model [11]. While this gives the CT+ model broad explanatory power, it remains challenging to establish whether any particular component mechanism definitively does contribute to a particular observation or that it definitively is ruled out.

The failure to demonstrate trans-sulcal WM (axonal) tension (observation 10 in Table 2) in ferret brain slices has been interpreted as inconsistent with the 'axonal tension hypothesis' in the original study [12] and in a number of subsequent studies and reviews (e.g., refs. [9,123,124]). However, there are objective grounds for qualifying this interpretation. (i) The original axonal tension hypothesis invoked tethering tension as well as pathway-specific tension, even though it emphasized the latter [3]. Since tissue cut observations 13, 14 in Table 2 provide strong evidence for tethering tension, only one of the two types of axonal tension proposed to mediate cortical folding is contested, rather than the axonal tension hypothesis as a whole, as others have also noted [64]. (ii) The apparent absence of one type of axonal tension (orthogonal to a white matter blade under a gyrus) in vitro in a single study in one species does not imply its absence in vivo in white matter blades in all species, including the special case of macaque V1 and V2 (observation 11). Similar to the above comment about the role of radial tension in regulating cortical thickness and expansion (observations 1–3), a parsimonious hypothesis is that pathway-specific axonal tension contributes to cortical folding in at least some regions in some species despite suggestive evidence to the contrary from a single experimental study.

3.6. Additional proposed mechanisms and observations

Other models and mechanisms for cortical folding have been proposed besides those evaluated in the preceding sections. Space limitations preclude a comprehensive analysis, but several additional mechanisms warrant brief consideration.

Stress-induced modulation of white matter growth. Several studies have explored variants of the differential tangential expansion mechanism in which mechanical stress induces volume changes in the subjacent SP/WM region. Using finite-element simulations to model the SP/WM as an isotropic visco-elastic tissue, Bayly et al. [125] found that the wavelength of folds increases with an increased tangential cortical growth rate or a decreased rate constant for stress-induced subcortical growth. Holland et al. [112] simulated anisotropic stress-induced axonal elongation using a continuum model of finite growth and reported that the initial fiber orientation can bias the location of buckling-induced folds. Garcia et al. [124] explored a model in which stress-induced tissue elongation modifies the underlying axonal orientation bias and reported that buckling increases the tangential orientation bias under sulcal fundi and the radial orientation bias under gyral crowns, consistent with experimental observations. These studies demonstrate progress in incorporating neurobiologically important characteristics into various mathematical simulations. Still missing, however, is a modeling and simulation framework that incorporates additional key neuroanatomical features such as the widespread occurrence of crossing fibers (i.e., multiple fiber bundles at different orientations at a given WM location) and the need to respect the topological continuity of individual axonal projections rather than fiber orientation biases that are independently computed for neighboring locations. Given that crossing fibers can be prominent in gyral WM blades (e.g., short-distance projections between sulcal banks separated by a gyral crown plus quasi-orthogonal projections between gyral cortex and distant cortical and subcortical targets [132], including the important special case of the gyral blade between macaque areas V1 and V2 (observation 11 in Table 2) it is vital to evaluate models that can represent this type of observed connectivity.

A specific concern arises from the statement [112] that "Axons Do Not Pull on the Brain—The Brain Pulls on the Axons". The authors further state: "When sensing mechanical stretch, axons quickly resume their new resting length and the stretch-induced axonal tension rapidly returns to its physiological baseline value. This suggests that—rather than axons pulling on the brain to induce cortical folding—the folding cortex pulls on the axons to trigger axonal elongation and white matter growth." That the brain indeed pulls on axons is not in dispute, nor is the presumption that this often leads to axonal elongation as the cortical mantle rapidly expands. However, the authors evidently take issue with the converse question of whether axons pull on the brain. Given that CNS axons can generate tension and that absent resting tension they retract until baseline tension is restored (see Section 1.3), it is plausible, and indeed seems highly likely that the above statements are both broadly correct (i.e., axons do pull on the brain, and the brain does pull on axons). Rather than framing the issues in terms of a questionable dichotomy, it may be more productive to focus on unresolved major questions of (i) to what degree does axonal tension contribute to the folding process overall, and (ii) to what degree does pathway-specific tension (Tenet 2 A of the CT+ model) contribute to specific gyral folds as distinct from tethering tension (Tenet 2B) contributing to buckling or irregular folding.

Another proposed mechanism involves 'anchoring' of nascent sulcal fundi to deeper structures, which is a plausible and intriguing hypothesis for some species such as the ferret [126,127] but seems unlikely to generalize to primates. A very different putative mechanism is the 'free energy' model [128], which proposes that cortical development follows a free energy gradient until reaching an energy minimum that also corresponds to a minimum aggregate wiring length. This model entails various assumptions that are implausible or unlikely (see SI Topic 8d of ref [1]. Finally, many studies have identified particular genes whose expression affects cortical folding, e.g., in conditions such as lissencephaly and polymicrogyria [9,129]; SI Topic 5 in ref. [1]. However, these are out of scope for this review, which has focused on mechanisms that can be expressed and evaluated in biomechanical terms.

3.7. Future directions

There are many exciting opportunities for further progress in studying the biomechanics of embryogenesis and nervous system morphogenesis in general and of cerebral cortical development and folding in particular. New methods and refinements of existing methods and tools may enable experimental measurements and perturbations that assess the forces and factors involved in morphogenesis with greater sensitivity and quantification than has heretofore been possible. With regard to cortical expansion and folding, a number of promising approaches have been suggested [1]. These include photoablation of cellular processes to test for tension in different locations and systems; analyses of gyrification in mouse mutants and in cerebral organoids; biomechanical measurements of tissue properties and cellular forces; and computational models that incorporate increasingly realistic constraints and features. An important overarching objective is to strive for models that are comprehensive rather than piecemeal and quantitative rather than qualitative.

Another high-level objective is to better understand the how the extraordinarily complex sets of biochemical reactions and molecular interactions involving thousands of genes, proteins, other macromolecules and regulatory molecules within each living cell are coordinated and orchestrated in space and time so as to generate the physical forces - tension and pressure – that actually change the shapes of cells and tissues. Elucidating how these myriad biochemical reactions and molecular signals impact specific morphogenetic events during healthy development and in developmental disorders represents a grand challenge for future generations of developmental neuroscientists.

Acknowledgments

I thank Kerry Grens for comments on the ms, Gregor Kasprian, Christine Haberler, and Nastasa Jovanov for constructive advice, and Anthony Bartley for assistance with figure preparation. This work was supported by the National Institutes of Health, USA (grant number MH060974).

Declarations of interest

None.

References

[1] D.C. Van Essen, A 2020 view of tension-based cortical morphogenesis, Proc. Natl. Acad. Sci. USA (2020), https://doi.org/10.1073/pnas.2016830117.
[2] S. Ramon y Cajal, Histologie du système nerveux de l'homme & des vertébrés, Maloine, Paris, 1909.
[3] D.C. Van Essen, A tension-based theory of morphogenesis and compact wiring in the central nervous system, Nature 385 (6614) (1997) 313–318, https://doi.org/10.1038/385313a0.
[4] C. Cherniak, Neural component placement, Trends Neurosci. 18 (12) (1995) 522–527, https://doi.org/10.1016/0166-2236(95)98373-7.
[5] C. Cherniak, Neural wiring optimization, Prog. Brain Res. 195 (2012) 361–371, https://doi.org/10.1016/B978-0-444-53860-4.00017-9.
[6] I.E. Wang, T.R. Clandinin, The influence of wiring economy on nervous system evolution, Curr. Biol. 26 (20) (2016) R1101–R1108, https://doi.org/10.1016/j.cub.2016.08.053.
[7] B.L. Chen, D.H. Hall, D.B. Chklovskii, Wiring optimization can relate neuronal structure and function, Proc. Natl. Acad. Sci. USA 103 (12) (2006) 4723–4728, https://doi.org/10.1073/pnas.0506806103.
[8] S. Ramon y Cajal, Textura del Sistema Nervioso del Hombre y de los Vertebrados trans, Nicolas Moya, Madrid, 1899.
[9] L. Del-Valle-Anton, V. Borrell, Folding brains: from development to disease modeling, Physiol. Rev. 102 (2) (2022) 511–550, https://doi.org/10.1152/physrev.00016.2021.
[10] I. Reillo, C. de Juan Romero, M.A. Garcia-Cabezas, V. Borrell, A role for intermediate radial glia in the tangential expansion of the mammalian cerebral cortex, Cereb. Cortex 21 (7) (2011) 1674–1694, https://doi.org/10.1093/cercor/bhq238.
[11] T. Tallinen, J.Y. Chung, F. Rousseau, N. Girard, J. Lefèvre, L. Mahadevan, On the growth and form of cortical convolutions, Nat. Phys. 12 (6) (2016) 588–593, https://doi.org/10.1038/nphys3632.
[12] G. Xu, A.K. Knutsen, K. Dikranian, C.D. Kroenke, P.V. Bayly, L.A. Taber, Axons pull on the brain, but tension does not drive cortical folding, J. Biomech. Eng. 132 (7) (2010), 071013, https://doi.org/10.1115/1.4001683.
[13] D.W. Thompson, On Growth and Form, Cambridge University Press, 1917.
[14] B. Fuller, Synergetics: Explorations in the Geometry of Thinking, McMillan, 1982.
[15] D.E. Ingber, N. Wang, D. Stamenovic, Tensegrity, cellular biophysics, and the mechanics of living systems, Rep. Prog. Phys. 77 (4) (2014), 046603, https://doi.org/10.1088/0034-4885/77/4/046603.
[16] M.E. Chicurel, C.S. Chen, D.E. Ingber, Cellular control lies in the balance of forces, Curr. Opin. Cell Biol. 10 (2) (1998) 232–239, https://doi.org/10.1016/s0955-0674(98)80145-2.
[17] H.W. Kroto, J.R. Heath, S.C. O'Brien, R.F. Curl, R.E. Smalley, C60: buckminsterfullerene, Nature 318 (1985) 182–183, https://doi.org/10.1038/318162a0.
[18] T. Mammoto, A. Mammoto, D.E. Ingber, Mechanobiology and developmental control, Annu Rev. Cell Dev. Biol. vol. 29 (2013) 27–61, https://doi.org/10.1146/annurev-cellbio-101512-122340.
[19] T. Mammoto, D.E. Ingber, Mechanical control of tissue and organ development, Development 137 (9) (2010) 1407–1420, https://doi.org/10.1242/dev.024166.
[20] T.D. Pollard, R.D. Goldman, Overview of the cytoskeleton from an evolutionary perspective, Cold Spring Harb. Perspect. Biol. 10 (7) (2018), https://doi.org/10.1101/cshperspect.a030288.
[21] A.F. Pegoraro, P. Janmey, D.A. Weitz, Mechanical properties of the cytoskeleton and cells, Cold Spring Harb. Perspect. Biol. 9 (2017), https://doi.org/10.1101/cshperspect.a022038.
[22] D.A. Fletcher, R.D. Mullins, Cell mechanics and the cytoskeleton, Nature 463 (7280) (2010) 485–492, https://doi.org/10.1038/nature08908.
[23] T. Hohmann, F. Dehghani, The cytoskeleton-a complex interacting meshwork, Cells 8 (2019) 4, https://doi.org/10.3390/cells8040362.
[24] A.P. Barnes, F. Polleux, Establishment of axon-dendrite polarity in developing neurons, Annu Rev. Neurosci. 32 (2009) 347–381, https://doi.org/10.1146/annurev.neuro.31.060407.125536.
[25] A. Fan, M.S.H. Joy, T. Saif, A connected cytoskeleton network generates axonal tension in embryonic Drosophila, Lab Chip 19 (18) (2019) 3133–3139, https://doi.org/10.1039/c9lc00243j.
[26] Q. Xiao, X. Hu, Z. Wei, K.Y. Tam, Cytoskeleton molecular motors: structures and their functions in neuron, Int J. Biol. Sci. 12 (9) (2016) 1083–1092, https://doi.org/10.7150/ijbs.15633.
[27] J.A. Hammer 3rd, W. Wagner, Functions of class V myosins in neurons, J. Biol. Chem. 288 (40) (2013) 28428–28434, https://doi.org/10.1074/jbc.R113.514497.
[28] D.B. Arnold, G. Gallo, Structure meets function: actin filaments and myosin motors in the axon, J. Neurochem 129 (2) (2014) 213–220, https://doi.org/10.1111/jnc.12503.
[29] N.C. Heer, A.C. Martin, Tension, contraction and tissue morphogenesis, Development 144 (23) (2017) 4249–4260, https://doi.org/10.1242/dev.151282.
[30] M.T. Kelliher, H.A. Saunders, J. Wildonger, Microtubule control of functional architecture in neurons, Curr. Opin. Neurobiol. 57 (2019) 39–45, https://doi.org/10.1016/j.conb.2019.01.003.
[31] A. Yuan, R.A. Nixon, Neurofilament proteins as biomarkers to monitor neurological diseases and the efficacy of therapies, Front Neurosci. 15 (2021), 689938, https://doi.org/10.3389/fnins.2021.689938.
[32] S. Kumar, X. Yin, B.D. Trapp, J.H. Hoh, M.E. Paulaitis, Relating interactions between neurofilaments to the structure of axonal neurofilament distributions through polymer brush models, Biophys. J. 82 (5) (2002) 2360–2372, https://doi.org/10.1016/S0006-3495(02)75581-1.
[33] J.Z. Kechagia, J. Ivaska, P. Roca-Cusachs, Integrins as biomechanical sensors of the microenvironment, Nat. Rev. Mol. Cell Biol. 20 (8) (2019) 457–473, https://doi.org/10.1038/s41580-019-0134-2.
[34] K.R. Long, W.B. Huttner, How the extracellular matrix shapes neural development, Open Biol. 9 (1) (2019), 180216, https://doi.org/10.1098/rsob.180216.
[35] A. Hartsock, W.J. Nelson, Adherens and tight junctions: structure, function and connections to the actin cytoskeleton, Biochim Biophys. Acta 1778 (3) (2008) 660, https://doi.org/10.1016/j.bbamem.2007.07.012.
[36] C.P. Brangwynne, et al., Microtubules can bear enhanced compressive loads in living cells because of lateral reinforcement, J. Cell Biol. 173 (5) (2006) 733–741, https://doi.org/10.1083/jcb.200601060.
[37] A. Gato, M.E. Desmond, Why the embryo still matters: CSF and the neuroepithelium as interdependent regulators of embryonic brain growth, morphogenesis and histiogenesis, Dev. Biol. 327 (2) (2009) 263–272, https://doi.org/10.1016/j.ydbio.2008.12.029.
[38] M. Prass, K. Jacobson, A. Mogilner, M. Radmacher, Direct measurement of the lamellipodial protrusive force in a migrating cell, J. Cell Biol. 174 (6) (2006) 767–772, https://doi.org/10.1083/jcb.200601159.
[39] M. Marin-Padilla, The human brain intracerebral microvascular system: development and structure, Front Neuroanat. 6 (2012) 38, https://doi.org/10.3389/fnana.2012.00038.
[40] A.I. Athamneh, D.M. Suter, Quantifying mechanical force in axonal growth and guidance, Front Cell Neurosci. 9 (2015) 359, https://doi.org/10.3389/fncel.2015.00359.
[41] N. Mandriota, C. Friedsam, J.A. Jones-Molina, K.V. Tatem, D.E. Ingber, O. Sahin, Cellular nanoscale stiffness patterns governed by intracellular forces, Nat. Mater. 18 (10) (2019) 1071–1077, https://doi.org/10.1038/s41563-019-0391-7.
[42] F. Basoli, et al., Biomechanical characterization at the cell scale: present and prospects, Front Physiol. 9 (2018) 1449, https://doi.org/10.3389/fphys.2018.01449.
[43] F. Serwane, et al., In vivo quantification of spatially varying mechanical properties in developing tissues, Nat. Methods 14 (2) (2017) 181–186, https://doi.org/10.1038/nmeth.4101.
[44] W.J. Polacheck, C.S. Chen, Measuring cell-generated forces: a guide to the available tools, Nat. Methods 13 (5) (2016) 415–423, https://doi.org/10.1038/nmeth.3834.
[45] E.W. Dent, S.L. Gupton, F.B. Gertler, The growth cone cytoskeleton in axon outgrowth and guidance, Cold Spring Harb. Perspect. Biol. 3 (3) (2011), https://doi.org/10.1101/cshperspect.a001800.
[46] J. Faix, K. Rottner, The making of filopodia, Curr. Opin. Cell Biol. 18 (1) (2006) 18–25, https://doi.org/10.1016/j.ceb.2005.11.002.
[47] C.E. Chan, D.J. Odde, Traction dynamics of filopodia on compliant substrates, Science 322 (5908) (2008) 1687–1691, https://doi.org/10.1126/science.1163595.
[48] K. Hu, L. Ji, K.T. Applegate, G. Danuser, C.M. Waterman-Storer, Differential transmission of actin motion within focal adhesions, Science 315 (5808) (2007) 111–115, https://doi.org/10.1126/science.1135085.
[49] J. Rajagopalan, A. Tofangchi, A.S. MT, Drosophila neurons actively regulate axonal tension in vivo, Biophys. J. 99 (10) (2010) 3208–3215, https://doi.org/10.1016/j.bpj.2010.09.029.
[50] L. Soares, M. Parisi, N.M. Bonini, Axon injury and regeneration in the adult Drosophila, Sci. Rep. 4 (2014) 6199, https://doi.org/10.1038/srep06199.
[51] B.G. Condron, K. Zinn, Regulated neurite tension as a mechanism for determination of neuronal arbor geometries in vivo, Curr. Biol. 7 (10) (1997) 813–816, https://doi.org/10.1016/s0960-9822(06)00343-5.
[52] J.N. Fass, D.J. Odde, Tensile force-dependent neurite elicitation via anti-beta1 integrin antibody-coated magnetic beads, Biophys. J. 85 (1) (2003) 623–636, https://doi.org/10.1016/S0006-3495(03)74506-8.
[53] P. Lamoureux, R.E. Buxbaum, S.R. Heidemann, Direct evidence that growth cones pull, Nature 340 (6229) (1989) 159–162, https://doi.org/10.1038/340159a0.
[54] T.J. Dennerll, H.C. Joshi, V.L. Steel, R.E. Buxbaum, S.R. Heidemann, Tension and compression in the cytoskeleton of PC-12 neurites. II: Quantitative measurements, J. Cell Biol. 107 (2) (1988) 665–674, https://doi.org/10.1083/jcb.107.2.665.
[55] M. O'Toole, P. Lamoureux, K.E. Miller, Measurement of subcellular force generation in neurons, Biophys. J. 108 (5) (2015) 1027–1037, https://doi.org/10.1016/j.bpj.2015.01.021.

[56] K. Franze, et al., Neurite branch retraction is caused by a threshold-dependent mechanical impact, Biophys. J. 97 (7) (2009) 1883–1890, https://doi.org/10.1016/j.bpj.2009.07.033.

[57] D.J. Odde, E.M. Tanaka, S.S. Hawkins, H.M. Buettner, Stochastic dynamics of the nerve growth cone and its microtubules during neurite outgrowth, Biotechnol. Bioeng. 50 (4) (1996) 452–461, https://doi.org/10.1002/(SICI)1097-0290(19960520)50:4<452::AID-BIT13>3.0.CO;2-L.

[58] B.J. Pfister, A. Iwata, D.F. Meaney, D.H. Smith, Extreme stretch growth of integrated axons, J. Neurosci. 24 (36) (2004) 7978–7983, https://doi.org/10.1523/JNEUROSCI.1974-04.2004.

[59] P. Lamoureux, S.R. Heidemann, N.R. Martzke, K.E. Miller, Growth and elongation within and along the axon, Dev. Neurobiol. 70 (3) (2010) 135–149, https://doi.org/10.1002/dneu.20764.

[60] W. Lu, M. Winding, M. Lakonishok, J. Wildonger, V.I. Gelfand, Microtubule-microtubule sliding by kinesin-1 is essential for normal cytoplasmic streaming in Drosophila oocytes, Proc. Natl. Acad. Sci. USA 113 (34) (2016) E4995–E5004, https://doi.org/10.1073/pnas.1522424113.

[61] U. Del Castillo, W. Lu, M. Winding, M. Lakonishok, V.I. Gelfand, Pavarotti/MKLP1 regulates microtubule sliding and neurite outgrowth in Drosophila neurons, Curr. Biol. 25 (2) (2015) 200–205, https://doi.org/10.1016/j.cub.2014.11.008.

[62] A. Goriely, The Mathematics and Mechanics of Biological Growth (Interdisciplinary applied mathematics, no. volume 45), Springer, New York, NY, 2017 pp. xxii, 646 pages.

[63] J. Nie, et al., Axonal fiber terminations concentrate on gyri, Cereb. Cortex 22 (12) (2012) 2831–2839, https://doi.org/10.1093/cercor/bhr361.

[64] G.F. Striedter, S. Srinivasan, E.S. Monuki, Cortical folding: when, where, how, and why? Annu Rev. Neurosci. 38 (2015) 291–307, https://doi.org/10.1146/annurev-neuro-071714-034128.

[65] E.K. Rodriguez, A. Hoger, A.D. McCulloch, Stress-dependent finite growth in soft elastic tissues, J. Biomech. 27 (4) (1994) 455–467, https://doi.org/10.1016/0021-9290(94)90021-3.

[66] D. Gilmour, M. Rembold, M. Leptin, From morphogen to morphogenesis and back, Nature 541 (7637) (2017) 311–320, https://doi.org/10.1038/nature21348.

[67] A.C. Martin, B. Goldstein, Apical constriction: themes and variations on a cellular mechanism driving morphogenesis, Development 141 (10) (2014) 1987–1998, https://doi.org/10.1242/dev.102228.

[68] N. Gorfinkiel, G.B. Blanchard, R.J. Adams, A. Martinez Arias, Mechanical control of global cell behaviour during dorsal closure in Drosophila, Development 136 (11) (2009) 1889–1898, https://doi.org/10.1242/dev.030866.

[69] J.D. Franke, R.A. Montague, D.P. Kiehart, Nonmuscle myosin II generates forces that transmit tension and drive contraction in multiple tissues during dorsal closure, Curr. Biol. 15 (24) (2005) 2208–2221, https://doi.org/10.1016/j.cub.2005.11.064.

[71] D.P. Kiehart, C.G. Galbraith, K.A. Edwards, W.L. Rickoll, R.A. Montague, Multiple forces contribute to cell sheet morphogenesis for dorsal closure in Drosophila, J. Cell Biol. 149 (2) (2000) 471–490, https://doi.org/10.1083/jcb.149.2.471.

[72] G.L. Galea, et al., Biomechanical coupling facilitates spinal neural tube closure in mouse embryos, Proc. Natl. Acad. Sci. USA 114 (26) (2017) E5177–E5186, https://doi.org/10.1073/pnas.1700934114.

[73] K.E. Garcia, R.J. Okamoto, P.V. Bayly, L.A. Taber, Contraction and stress-dependent growth shape the forebrain of the early chicken embryo, J. Mech. Behav. Biomed. Mater. 65 (2017) 383–397, https://doi.org/10.1016/j.jmbbm.2016.08.010.

[74] T. Nishimura, H. Honda, M. Takeichi, Planar cell polarity links axes of spatial dynamics in neural-tube closure, Cell 149 (5) (2012) 1084–1097, https://doi.org/10.1016/j.cell.2012.04.021.

[75] E. Nikolopoulou, G.L. Galea, A. Rolo, N.D. Greene, A.J. Copp, Neural tube closure: cellular, molecular and biomechanical mechanisms, Development 144 (4) (2017) 552–566, https://doi.org/10.1242/dev.145904.

[76] H. Hashimoto, F.B. Robin, K.M. Sherrard, E.M. Munro, Sequential contraction and exchange of apical junctions drives zippering and neural tube closure in a simple chordate, Dev. Cell 32 (2) (2015) 241–255, https://doi.org/10.1016/j.devcel.2014.12.017.

[77] M.E. Desmond, A.G. Jacobson, Embryonic brain enlargement requires cerebrospinal fluid pressure, Dev. Biol. 57 (1) (1977) 188–198, https://doi.org/10.1016/0012-1606(77)90364-5.

[78] M.E. Desmond, M.L. Levitan, A.R. Haas, Internal luminal pressure during early chick embryonic brain growth: descriptive and empirical observations, Anat. Rec. A Disco Mol. Cell Evol. Biol. 285 (2) (2005) 737–747, https://doi.org/10.1002/ar.a.20211.

[79] B.A. Filas, A. Oltean, S. Majidi, P.V. Bayly, D.C. Beebe, L.A. Taber, Regional differences in actomyosin contraction shape the primary vesicles in the embryonic chicken brain, Phys. Biol. 9 (6) (2012), 066007, https://doi.org/10.1088/1478-3975/9/6/066007.

[80] K.E. Garcia, W.G. Stewart, M.G. Espinosa, J.P. Gleghorn, L.A. Taber, Molecular and mechanical signals determine morphogenesis of the cerebral hemispheres in the chicken embryo, Development 146 (2019), https://doi.org/10.1242/dev.174318.

[81] B. Mota, et al., White matter volume and white/gray matter ratio in mammalian species as a consequence of the universal scaling of cortical folding, Proc. Natl. Acad. Sci. USA 116 (30) (2019) 15253–15261, https://doi.org/10.1073/pnas.1716956116.

[82] S.A. Bayer, J. Altman, The Human Brain During the Late First Trimester (Atlas of Human Central Nervous System Development), CRC Press, 2006.

[83] I. Kostovic, P. Rakic, Developmental history of the transient subplate zone in the visual and somatosensory cortex of the macaque monkey and human brain, J. Comp. Neurol. 297 (3) (1990) 441–470, https://doi.org/10.1002/cne.902970309.

[84] P. Rakic, Neurons in rhesus monkey visual cortex: systematic relation between time of origin and eventual disposition, Science 183 (4123) (1974) 425–427, https://doi.org/10.1126/science.183.4123.425.

[85] C. Dehay, P. Giroud, M. Berland, I. Smart, H. Kennedy, Modulation of the cell cycle contributes to the parcellation of the primate visual cortex, Nature 366 (6454) (1993) 464–466, https://doi.org/10.1038/366464a0.

[86] I. Kostovic, G. Sedmak, M. Judas, Neural histology and neurogenesis of the human fetal and infant brain, Neuroimage 188 (2019) 743–773, https://doi.org/10.1016/j.neuroimage.2018.12.043.

[87] T.J. Nowakowski, A.A. Pollen, C. Sandoval-Espinosa, A.R. Kriegstein, Transformation of the radial glia scaffold demarcates two stages of human cerebral cortex development, Neuron 91 (6) (2016) 1219–1227, https://doi.org/10.1016/j.neuron.2016.09.005.

[88] E. Taverna, M. Gotz, W.B. Huttner, The cell biology of neurogenesis: toward an understanding of the development and evolution of the neocortex, Annu Rev. Cell Dev. Biol. 30 (2014) 465–502, https://doi.org/10.1146/annurev-cellbio-101011-155801.

[89] I. Bystron, P. Rakic, Z. Molnar, C. Blakemore, The first neurons of the human cerebral cortex, Nat. Neurosci. 9 (7) (2006) 880–886, https://doi.org/10.1038/nn1726.

[90] K. Sekine, T. Honda, T. Kawauchi, K. Kubo, K. Nakajima, The outermost region of the developing cortical plate is crucial for both the switch of the radial migration mode and the Dab1-dependent “inside-out” lamination in the neocortex, J. Neurosci. 31 (25) (2011) 9426–9439, https://doi.org/10.1523/JNEUROSCI.0650-11.2011.

[91] A. Batardiere, et al., Early specification of the hierarchical organization of visual cortical areas in the macaque monkey, Cereb. Cortex 12 (5) (2002) 453–465, https://doi.org/10.1093/cercor/12.5.453.

[92] T.A. Coogan, D.C. Van Essen, Development of connections within and between areas V1 and V2 of macaque monkeys, J. Comp. Neurol. 372 (3) (1996) 327–342, https://doi.org/10.1002/(SICI)1096-9861(19960826)372:3<327::AID-CNE1>3.0.CO;2-4.

[93] X. Wang, D.R. Pettersson, C. Studholme, C.D. Kroenke, Characterization of laminar zones in the mid-gestation primate brain with magnetic resonance imaging and histological methods, Front Neuroanat. 9 (2015) 147, https://doi.org/10.3389/fnana.2015.00147.

[94] X. Wang, C. Studholme, P.L. Grigsby, A.E. Frias, V.C. Cuzon Carlson, C. D. Kroenke, Folding, but not surface area expansion, is associated with cellular morphological maturation in the fetal cerebral cortex, J. Neurosci. 37 (8) (2017) 1971–1983, https://doi.org/10.1523/JNEUROSCI.3157-16.2017.

[95] Z. Liu, X. Wang, N. Newman, K.A. Grant, C. Studholme, C.D. Kroenke, Anatomical and diffusion MRI brain atlases of the fetal rhesus macaque brain at 85, 110 and 135 days gestation, Neuroimage 206 (2020), 116310, https://doi.org/10.1016/j.neuroimage.2019.116310.

[96] N.T. Markov, et al., A weighted and directed interareal connectivity matrix for macaque cerebral cortex, Cereb. Cortex 24 (1) (2014) 17–36, https://doi.org/10.1093/cercor/bhs270.

[97] S.A. Bayer, J. Altman, The Human Brain during the Second Trimester (Atlas of Human Central Nervous System Development), CRC Press, 2005.

[98] E. Gonzalez-Arnay, M. Gonzalez-Gomez, G. Meyer, A radial glia fascicle leads principal neurons from the pallial-subpallial boundary into the developing human insula, Front Neuroanat. 11 (2017) 111, https://doi.org/10.3389/fnana.2017.00111.

[99] A. Feess-Higgins, J-C. Larroche, Development of the Human Fetal Brain: An Anatomical Atlas, Masson, Paris, 1988, p. 200.

[100] D. Prayer, et al., MRI of normal fetal brain development, Eur. J. Radio. 57 (2) (2006) 199–216, https://doi.org/10.1016/j.ejrad.2005.11.020.

[101] S. Budday, C. Raybaud, E. Kuhl, A mechanical model predicts morphological abnormalities in the developing human brain, Sci. Rep. 4 (2014) 5644, https://doi.org/10.1038/srep05644.

[102] M.F. Glasser, et al., A multi-modal parcellation of human cerebral cortex, Nature 536 (7615) (2016) 171–178, https://doi.org/10.1038/nature18933.

[103] F. Wang, et al., Developmental topography of cortical thickness during infancy, Proc. Natl. Acad. Sci. USA 116 (32) (2019) 15855–15860, https://doi.org/10.1073/pnas.1821523116.

[104] V. Borrell, How cells fold the cerebral cortex, J. Neurosci. 38 (4) (2018) 776–783, https://doi.org/10.1523/JNEUROSCI.1106-17.2017.

[105] C. Llinares-Benadero, V. Borrell, Deconstructing cortical folding: genetic, cellular and mechanical determinants, Nat. Rev. Neurosci. 20 (3) (2019) 161–176, https://doi.org/10.1038/s41583-018-0112-2.

[106] L. Siklos, U. Kuhnt, A. Parducz, P. Szerdahelyi, Intracellular calcium redistribution accompanies changes in total tissue Na+, K+ and water during the first two hours of in vitro incubation of hippocampal slices, Neuroscience 79 (4) (1997) 1013–1022, https://doi.org/10.1016/s0306-4522(97)00031-6.

[107] A. Kriegstein, S. Noctor, V. Martinez-Cerdeno, Patterns of neural stem and progenitor cell division may underlie evolutionary cortical expansion,", Nat. Rev. Neurosci. 7 (11) (2006) 883–890, https://doi.org/10.1038/nrn2008.

[108] S.A. Bayer, J. Altman, The Human Brain During the Third Trimester (Atlas of Human Central Nervous System Development), CRC Press, 2003.

[109] D.C. Van Essen, Cause and effect in cortical folding, Nat. Rev. Neurosci. (2007), https://doi.org/10.1038/nrn2008-c1.

[110] D.H. Barron, An experimental analysis of some factors involved in the development of the fissure pattern of the cerebral cortex, J. Exp. Zool. 113 (1950) 553–581.
[111] S. Wilson, et al., Development of human white matter pathways in utero over the second and third trimester, Proc. Natl. Acad. Sci. USA 118 (20) (2021), https://doi.org/10.1073/pnas.2023598118.
[112] M.A. Holland, K.E. Miller, E. Kuhl, Emerging brain morphologies from axonal elongation, Ann. Biomed. Eng. 43 (7) (2015) 1640–1653, https://doi.org/10.1007/s10439-015-1312-9.
[113] C.C. Hilgetag, H. Barbas, Role of mechanical factors in the morphology of the primate cerebral cortex, PLoS Comput. Biol. 2 (3) (2006), e22, https://doi.org/10.1371/journal.pcbi.0020022.
[114] V.A. Klyachko, C.F. Stevens, Connectivity optimization and the positioning of cortical areas, Proc. Natl. Acad. Sci. USA 100 (13) (2003) 7937–7941, https://doi.org/10.1073/pnas.0932745100.
[115] M. Ercsey-Ravasz, et al., A predictive network model of cerebral cortical connectivity based on a distance rule, Neuron 80 (1) (2013) 184–197, https://doi.org/10.1016/j.neuron.2013.07.036.
[117] D.C. Van Essen, W.T. Newsome, J.H. Maunsell, J.L. Bixby, The projections from striate cortex (V1) to areas V2 and V3 in the macaque monkey: asymmetries, areal boundaries, and patchy connections, J. Comp. Neurol. 244 (4) (1986) 451–480, https://doi.org/10.1002/cne.902440405.
[118] K.S. Ono M, CD Abernathey, Atlas of the Cerebral Sulci, Thieme Medical Publishers, Inc., New York, 1990.
[119] K.R. Long, et al., Extracellular matrix components HAPLN1, lumican, and collagen I cause hyaluronic acid-dependent folding of the developing human neocortex, e6, Neuron 99 (4) (2018) 702–719, https://doi.org/10.1016/j.neuron.2018.07.013.
[120] G. Xu, P.V. Bayly, L.A. Taber, Residual stress in the adult mouse brain, Biomech. Model Mechanobiol. 8 (4) (2009) 253–262, https://doi.org/10.1007/s10237-008-0131-4.
[121] I. Ferrer, I. Fabregues, E. Condom, A Golgi study of the sixth layer of the cerebral cortex. II. The gyrencephalic brain of Carnivora, Artiodactyla and Primates, J. Anat. 146 (1986) 87–104. ⟨https://www.ncbi.nlm.nih.gov/pubmed/3693064⟩.
[122] I.H. Smart, G.M. McSherry, Gyrus formation in the cerebral cortex of the ferret. II. Description of the internal histological changes, J. Anat. 147 (1986) 27–43. ⟨https://www.ncbi.nlm.nih.gov/pubmed/3693076⟩.
[123] L. Ronan, P.C. Fletcher, From genes to folds: a review of cortical gyrification theory, Brain Struct. Funct. 220 (5) (2015) 2475–2483, https://doi.org/10.1007/s00429-014-0961-z.
[124] K.E. Garcia, X. Wang, C.D. Kroenke, A model of tension-induced fiber growth predicts white matter organization during brain folding, Nat. Commun. 12 (1) (2021) 6681, https://doi.org/10.1038/s41467-021-26971-9.
[125] P.V. Bayly, R.J. Okamoto, G. Xu, Y. Shi, L.A. Taber, A cortical folding model incorporating stress-dependent growth explains gyral wavelengths and stress patterns in the developing brain, Phys. Biol. 10 (1) (2013), 016005, https://doi.org/10.1088/1478-3975/10/1/016005.
[126] I.H. Smart, G.M. McSherry, Gyrus formation in the cerebral cortex in the ferret. I. Description of the external changes, J. Anat. 146 (1986) 141–152. ⟨https://www.ncbi.nlm.nih.gov/pubmed/3693054⟩.
[127] S. Rana, R. Shishegar, S. Quezada, L. Johnston, D.W. Walker, M. Tolcos, The subplate: a potential driver of cortical folding? Cereb. Cortex 29 (11) (2019) 4697–4708, https://doi.org/10.1093/cercor/bhz003.
[128] B. Mota, S. Herculano-Houzel, BRAIN STRUCTURE. Cortical folding scales universally with surface area and thickness, not number of neurons, Science 349 (6243) (2015) 74–77, https://doi.org/10.1126/science.aaa9101.
[129] Y. Shinmyo, et al., Folding of the cerebral cortex requires Cdk5 in upper-layer neurons in gyrencephalic mammals, Cell Rep. 20 (9) (2017) 2131–2143, https://doi.org/10.1016/j.celrep.2017.08.024.
[130] S. De Vincentiis, A. Falconieri, M. Mainardi, V. Cappello, V. Scribano, R. Bizzarri, B. Storti, L. Dente, M. Costa, V. Raffa. Extremely Low Forces Induce Extreme Axon Growth. J Neurosci. 40 (26) (2020) 4997-5007. doi: 10.1523/JNEUROSCI.3075-19.2020.
[131] C.D. Kroenke, P.V. Bayly, How Forces Fold the Cerebral Cortex, J Neurosci 38 (4) (2018) 767–775, https://doi.org/10.1523/JNEUROSCI.1105-17.2017.
[132] D.C. Van Essen, S. Jbabdi, S.N. Sotiropoulos, C. Chen, K. Dikranian, T. Coalson, J. Harwell, T.E. Behrens, M.F. Glasser, Mapping connections in humans and non-human primates: aspirations and challenges for diffusion imaging. Diffusion MRI, 2nd, Academic Press, 2014, pp. 337–358.